Dielectric nanoantennas to manipulate solid-state light emission

Sébastien Bidault, Mathieu Mivelle Mivelle, Nicolas Bonod

Journal of Applied Physics

Dielectric nanoantennas to manipulate solid-state light emission

Cite as: J. Appl. Phys. **126**, 094104 (2019); https://doi.org/10.1063/1.5108641
Submitted: 30 April 2019 . Accepted: 07 August 2019 . Published Online: 06 September 2019

Sébastien Bidault, Mathieu Mivelle, and Nicolas Bonod

Journal of Applied Physics PERSPECTIVE scitation.org/journal/jap

Dielectric nanoantennas to manipulate solid-state light emission

Cite as: J. Appl. Phys. **126**, 094104 (2019); doi: 10.1063/1.5108641
Submitted: 30 April 2019 · Accepted: 7 August 2019 ·
Published Online: 6 September 2019

View Online Export Citation CrossMark

Sébastien Bidault,[1,a)] Mathieu Mivelle,[2] and Nicolas Bonod[3,b)]

AFFILIATIONS

[1]Institut Langevin, ESPCI Paris, CNRS, PSL University, 75005 Paris, France
[2]Sorbonne Université, CNRS, Institut des NanoSciences de Paris, 75005 Paris, France
[3]Aix Marseille Univ, CNRS, Centrale Marseille, Institut Fresnel, 13013 Marseille, France

Note: This paper is part of the Special Topic on Dielectric Nanoresonators and Metamaterials.

[a)]**Electronic mail:** sebastien.bidault@espci.fr
[b)]**Electronic mail:** nicolas.bonod@fresnel.fr

ABSTRACT

Thanks to their enhanced and confined optical near-fields, broadband subwavelength resonators have the ability to enhance the spontaneous emission rate and brightness of solid-state emitters at room temperature. Over the last few years, high-index dielectrics have emerged as an alternative platform to plasmonic materials in order to design nanoresonators/optical nanoantennas with low ohmic losses. In particular, the excitation of electric and magnetic multipolar modes in dielectric resonators provides numerous degrees of freedom to manipulate the directivity and radiative decay rates of electric or magnetic quantum emitters. We review recent theoretical and experimental applications of dielectric nanoantennas to enhance or control decay rates of both electric and magnetic emitters but also to manipulate their radiation pattern through the coherent excitation of electric and magnetic modes; before discussing perspectives of this emerging field.

I. INTRODUCTION

The theoretical demonstration in 2010[1] and 2011[2]—followed by experimental proof in 2012[3,4]—that silicon subwavelength spheres feature broadband electric and magnetic multipolar resonances in the visible and near infrared range triggered an intense research activity in the development of optically resonant nanostructures made from high-index dielectrics. In particular, creating broadband nanoscale resonators using materials with low-ohmic losses combines the advantages of plasmonic systems to interact with quantum emitters at room temperature and of dielectric cavities to manipulate radiative optical modes without introducing nonradiative decay channels. Moreover, by featuring intense electric field gradients and curls inside the dielectric material, these nanoresonators provide new degrees of freedom to design optical antennas by offering multipolar electric and magnetic modes with larger quality factors than plasmonic systems. All of these phenomena explain the current interest in tuning spontaneous emission processes from solid-state light sources at room temperature using high-index nanostructures, in order to improve the brightness and directivity of emission but also to manipulate spontaneous decay rates.

In the first part of this perspective, we highlight the specific properties of dielectric nanoresonators compared to their plasmonic counterparts and introduce briefly the basic working principles of optical nanoantennas to manipulate spontaneous emission from either electric or magnetic quantum emitters. Since this perspective is focused on the coupling between optical resonators and solid-state emitters at room temperature where electron-phonon interactions lead to homogeneously broadened luminescence spectra, we do not compare the properties of dielectric nanoantennas to dielectric microcavities that have been extensively used to influence spontaneous emission at cryogenic temperatures.[5–9] Moreover, several review articles have discussed the specificities of plasmonic nanoantennas to control spontaneous emission with respect to dielectric microcavities.[10–12]

In the last paragraphs of this perspective, we analyze and review recent results from the literature, in particular, the optimization of emission directivity and the enhancement or inhibition of

luminescence properties. The first part is devoted to the design of directive antennas, where we emphasize the interest of inducing coherent electric and magnetic modes in dielectric resonators that interfere in the far-field. The last paragraphs of this perspective focus on the manipulation of spontaneous decay channels, first reviewing recent results on the enhancement of luminescence from solid-state emitters before highlighting the full potential of dielectric antennas to inhibit spontaneous emission or to manipulate magnetic or chiral emitters.

II. FROM PLASMONIC MATERIALS TO HIGH-INDEX DIELECTRICS TO DESIGN NANOANTENNAS

When discussing the plasmon resonances of nanoparticles, a quasistatic approximation is generally used in order to derive the polarizability of the particle and explain the resonant behavior of its extinction cross section. This leads to the famous relationship between the polarizability α_0 of a spherical particle of radius a with the dispersive dielectric constant of the plasmonic material ε_m and of its environment ε_d,

$$\alpha_0(\lambda) = 4\pi a^3 \frac{\varepsilon_m(\lambda) - \varepsilon_d}{\varepsilon_m(\lambda) + 2\varepsilon_d}. \quad (1)$$

For spheres, but also for other particle geometries, a resonant polarizability at visible frequencies is then only observed for materials that feature negative real parts of their dielectric constant at these wavelengths, namely, plasmonic materials with quasifree electrons (which can generally be described using a Drude model). It is important to stress that calculating the polarizability of a nanoparticle in the quasistatic approximation implies that this particle does not scatter light in order to verify the optical theorem.[13] Therefore, Eq. (1) cannot generally be applied to plasmonic nanoparticles unless their scattering cross section is negligible with respect to their absorption cross section, namely, for gold or silver particles with diameters below 10 nm. Outside of photothermal applications, resonant particles with negligible scattering cross sections have a limited range of applications. On the contrary, in order to design optical nanoantennas capable of enhancing the emission of solid-state light sources, producing nanoscale resonators that efficiently radiate energy to the far-field is a crucial requirement.

A depolarization factor is generally introduced in the quasistatic particle polarizability in order to correct for radiative damping.[13–16] This term allows the definition of a dipolar approximation for the optical response of resonant nanoparticles that verifies the optical theorem. However, this approximation rapidly breaks down when considering resonator sizes typically used in nanophotonics. A full multipolar description is then necessary to correctly describe the optical response of nanostructures; using, for instance, Mie theory in the case of spherical systems. Importantly, when the quasistatic approximation breaks down, the requirement that the nanoparticle must be made of a material with a negative dielectric constant in order to obtain a resonant optical response is no longer true. This means that nanoscale resonators made from dielectric materials, with a high positive dielectric constant with respect to the environment, can feature dipolar and multipolar resonances at visible and near-infrared frequencies.[16,17]

With the rapid development of resonant particles made of high-index dielectrics, it is interesting to consider the main differences in the optical response of plasmonic and dielectric resonators. In the case of spherical particles, it is possible to highlight them using Mie theory. Recently, it was demonstrated that a dielectric sphere of dispersive permittivity ε_{eq} can mimic the electric dipolar resonant behavior of a plasmonic sphere of dielectric constant ε_m with the same radius a if[17]

$$\varepsilon_{eq}(\lambda) \approx \left(\frac{9\lambda}{4\pi a}\right)^2 \frac{1 - (4\pi a/9\lambda)^2 \varepsilon_m(\lambda)}{1 - 2(4\pi a/9\lambda)^2 \varepsilon_m(\lambda)}. \quad (2)$$

This equation demonstrates that, if the particle radius is infinitely smaller than the wavelength of light, ε_{eq} shoots toward infinity, verifying that nanoparticles made of materials with positive permittivities cannot feature resonances in the quasistatic approximation. Since the accessible dielectric constants at visible wavelengths remain below 30, compared to values of several hundreds at radiofrequencies, this equation also explains why dipolar electric resonances in high-index dielectrics are typically observed with dimensions larger than $\lambda/10$.

To highlight some of the similarities and discrepancies in the optical response of dielectric and plasmonic nanoscale resonators, Fig. 1(a) displays the local field enhancements of the electric and magnetic fields in dimers of silicon and gold nanospheres. We observe that the distributions of the electric field in the surrounding medium are similar with a strong local enhancement in the gap between spheres. However, while the skin depth of noble metals render the electric and magnetic fields negligible inside the gold nanospheres, these fields can exhibit strong amplitudes inside the silicon spheres. In summary, while plasmonic materials have the added bonus of providing optical resonances for deeply subwavelength particles, high-index dielectrics provide numerous advantages and new degrees of freedom to design nanoscale resonators. Indeed, their ability to feature broadband resonances at visible wavelengths with strong internal fields opens numerous exciting possibilities:

(i) Strong gradients and curls of the electric field inside the resonator allow the excitation of multipolar magnetic resonances in addition to their electric counterpart. This phenomenon requires complex nanostructure geometries in plasmonics, such as split-ring resonators, while it is directly observed for spheres with dielectrics. In the context of this perspective, magnetic multipolar modes are particularly important to control spontaneous decay processes from emitters featuring magnetic transition dipoles (such as rare-earth ions[18]) or to design directive nanoantennas.

(ii) Weak imaginary parts of the dielectric constant for numerous high-index dielectrics mean that their multipolar modes will be dominated by radiative damping processes. This provides new design strategies for dielectric resonators by considering higher order modes. Indeed, in plasmonics, all modes apart from the electric dipole are generally dominated by ohmic losses. This phenomenon can be observed in Fig. 1(b) where an emitter longitudinally coupled to the dipolar mode of a gold nanosphere dimer exhibits a strong increase of its decay

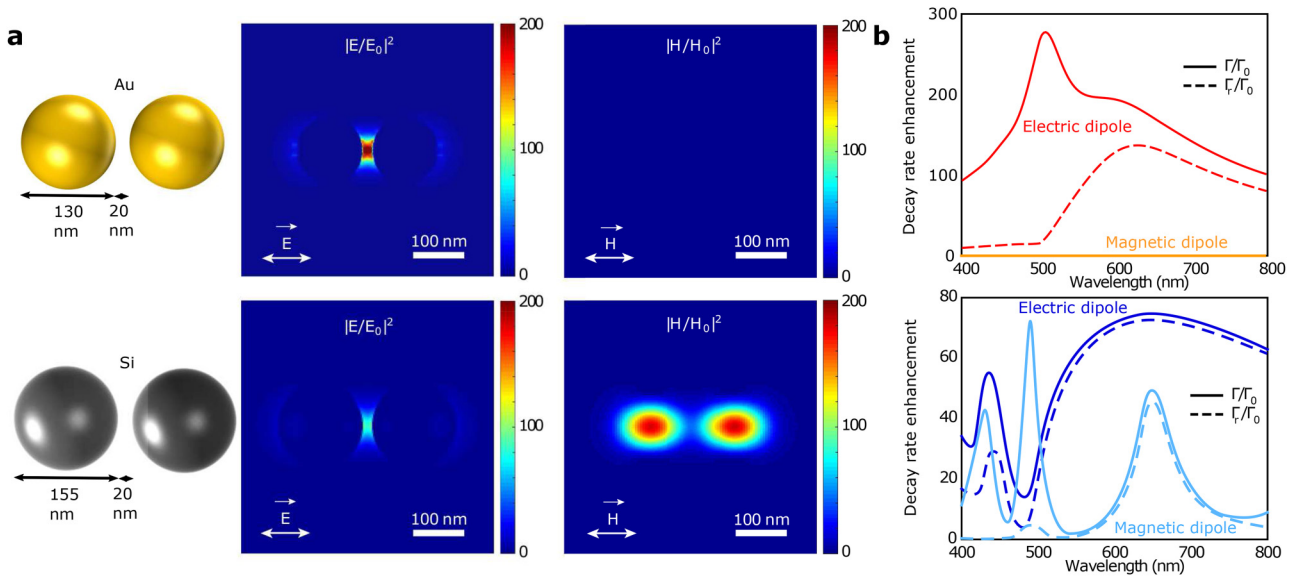

FIG. 1. Comparison between gold and silicon-based nanoantennas made of coupled spheres. (a) Considered dimer geometries (optimized to maximize the electric field in the center of a 20 nm gap at 650 nm in air) and simulated electric and magnetic field distributions for a longitudinally polarized excitation. (b) Simulated total (solid lines) and radiative (dashed lines) decay rate changes for electric and magnetic dipolar emitters, longitudinally coupled to the same dimer antennas and positioned in the centre of the 20 nm gap.

rate dominated by radiative processes; while a higher order mode mainly leads to a strong increase of the nonradiative decay rate. But for high-index dielectrics, high-order modes can remain radiative modes but with much higher quality factors than the electric dipole [see, for instance, in Fig. 1(b), the influence of electric dipolar and quadrupolar modes of a silicon nanosphere dimer coupled longitudinally to a source electric dipole: radiative processes remain important for the higher order mode]. Importantly, near-field light sources, such as quantum emitters, which couple to these resonators will mainly interact with radiative modes. This is important to optimize the quantum yield of the coupled emitter and truly essential when designing an antenna capable of inhibiting spontaneous emission, phenomenon for which nonradiative decay channels must be prevented.

(iii) More generally, strong internal fields in a material that can be luminescent or exhibit a nonlinear permittivity provide novel design strategies for optimized and fully integrated nanophotonic platforms.

III. WORKING PRINCIPLES OF OPTICAL NANOANTENNAS

A. Analogy with radiofrequency antennas

Over the last fifteen years, the coupling between quantum emitters and nanoscale optical resonators has been actively studied and pursued in order to optimize spontaneous photon emission, essentially using plasmonic systems.[19,20] A parallel was rapidly drawn between this interaction and radiofrequency antennas which are designed to optimize the power radiated by a subwavelength electric dipolar source.[21] In practice, both optical nanoresonators and radiofrequency antennas are designed to increase the local density of electromagnetic modes to which a point dipolar source can couple in the near-field in order to radiate efficiently in the far-field.[22]

In a weak coupling regime between the emitter and the resonator,[23] this analogy goes even further when considering the evolution of the spontaneous decay rate Γ of the emitter using Fermi's golden rule[24]

$$\Gamma = \frac{2}{3\hbar\varepsilon_0}\omega|\tilde{\mathbf{p}}|^2\rho(\mathbf{r},\omega), \tag{3}$$

with $\tilde{\mathbf{p}}$ the electric dipole moment operator of the emitter between its excited and ground states, and $\rho(\mathbf{r},\omega)$ the local density of optical states (LDOS) at the position $\mathbf{r}$ of the emitter and for a frequency ω. The LDOS involves the total electric field at the position of the emitter, which is the sum of the field emitted by the dipole $\mathbf{E_p}(\mathbf{r})$ and the backscattered field, i.e., the field scattered back to the emitter by the inhomogeneous environment $\mathbf{E_s}(\mathbf{r})$.[23] In the case of a homogeneous medium of permittivity ε, only the emitted field should be considered. This allows the derivation of the relative change of total decay rate as

$$\frac{\Gamma}{\Gamma_0} = 1 + \eta_0\frac{6\pi\varepsilon}{|\tilde{\mathbf{p}}|^2}\frac{1}{k^3}Im(\tilde{\mathbf{p}}^*.E_s(r)), \tag{4}$$

where $\eta_0 = \Gamma_{R_0}/\Gamma_0$ is the intrinsic quantum yield of the quantum emitter with Γ_{R_0} the radiative decay rate of the emitter in a

homogeneous environment. Importantly, when computing the relative change of the power P dissipated by a classical electric dipole $\mathbf{p}$ in an inhomogeneous environment, compared to the power radiated in the homogeneous case P_0, a similar equation is obtained,[25]

$$\frac{P}{P_0} = 1 + \frac{6\pi\varepsilon}{|\mathbf{p}|^2}\frac{1}{k^3} Im(\mathbf{p}^*.\mathbf{E_s}(\mathbf{r})). \quad (5)$$

These equations show nicely how the relative change of a purely quantum mechanical process, spontaneous photon decay, can be directly computed using electrodynamic calculations. Let us stress that even though these two expressions are similar, they describe two distinct phenomena. Γ describes the transition probability between two energy electronic levels, triggered by quantum fluctuations, and follows Fermi's golden rule. On the other side, P describes the power dissipated by a classical harmonic dipole. However, the analogy between these quantum and classical descriptions is striking and allows classical descriptions of purely quantum process.[24] This is an important aspect of nanophotonics, which deal with quantum light-matter interactions that are generally manipulated in a purely classical way by engineering the local density of electromagnetic states, and further explains the analogy between radiofrequency and optical antennas.[26] Several differences should however be stressed as, in radiofrequency antennas, ohmic losses are generally very weak compared to radiation damping. This is not true in optical nanoantennas because both the emitter and the resonator feature nonradiative decay channels. For instance, the initial quantum yield of emitters, η_0, is always below 1. η_0 is the only difference between Eqs. (4) and (5) and the comparison between classical electrodynamic calculations and fluorescence measurements should always carefully consider the initial yield. Furthermore, most materials considered for optical antennas have nonnegligible imaginary parts of their permittivity, introducing ohmic dissipation in the resonator. This is one of the strengths of high-index dielectrics compared to plasmonic systems for nanoantennas.

It is important to note that the interaction term $Im(\tilde{\mathbf{p}}^*.E_s)$ between the emitter and electromagnetic field in Eq. (4) involves only the electric transition dipolar operator $\tilde{\mathbf{p}}$. However, in a more general case, the interaction involves the magnetic transition dipole (that couples to the magnetic component of light) and the electric quadrupole, that is, involved when the gradient of the electric field at the position of the emitter cannot be neglected.

For a homogeneous environment, a dipolar approximation is reasonable since the size of the quantum emitter is much smaller than the wavelength. The curl and the gradient of the electric field are, therefore, negligible at the scale of the emitter leading to negligible magnetic dipole and electric quadrupole components of the interaction Hamiltonian. This approximation is not valid for emitters whose electric dipole transition is symmetry forbidden (such as rare-earth cations) leading to electric dipole and magnetic dipole transitions of similar amplitude.[27]

Furthermore, in the vicinity of optical resonators, the curl and gradient of the electric field can be nonnegligible, making the dipole approximation no longer valid.[28–30] Importantly, in the case of the magnetic transition dipole, a similar derivation can be inferred using Fermi's golden rule and equivalent equations to Eqs. (4) and (5) can be obtained when considering a classical magnetic dipole source.[31–35]

Figure 1(b) provides the simulated modification of radiative and total decay rates of electric and magnetic emitters in the center of silicon or gold nanosphere dimers. These data show clearly the ability of dielectric antennas to manipulate the properties of solid-state light sources whose emission is mediated by either electric or magnetic transition dipoles,[32,33] while spherical plasmonic antennas only influence electric emitters. Furthermore, these simulations highlight the low ohmic losses of dielectric resonators as the radiative and total decay rates changes are nearly superimposed for the low-order red-sifted longitudinal dipolar modes. These data also evidence the influence of the considered antenna resonance on the emission efficiency of the coupled emitter-antenna system: the magnetic dipolar mode, which couples less efficiently to the far-field than the more radiatively damped electric dipolar mode (leading to a higher quality factor), features larger nonradiative decay rates since the absorption of silicon at 650 nm is not fully negligible. We finally observe that the high-order modes between 400 nm and 500 nm in a silicon nanosphere dimer still feature strong nonradiative losses: this is because these wavelengths remain significantly below the bandgap of silicon. In order to exploit high-order modes to modify spontaneous decay rates without ohmic losses in high-index dielectrics, it is essential to work above the bandgap of the considered material because of the large quality factors of high-order modes.

B. Enhancing luminescence signals with nanoantennas

If we consider the analogy with radiofrequency antennas further, nanoscale resonators should be able to not only influence spontaneous decay rates but also the excitation rate of the emitter or the emission directivity since radiofrequency antennas are well known to enhance signal reception and to be strongly directional.

Concerning the excitation rate, reciprocity in electromagnetism implies that, if an antenna can enhance the radiative emission rate in the far-field, it will also enhance its excitation rate in the near-field when considering the same wavelength of light and opposite propagation wave-vectors.[36,37] Qualitatively, one can understand that, if an antenna features channels to which an emitter can couple in the near-field to radiate energy in the far-field; then a far-field electromagnetic wave can also couple to these same channels in order to efficiently excite the emitter. This is no longer valid for the nonradiative modes to which the emitter can couple. Overall, this increase in excitation leads to the well-known local field enhancements or hot-spots in the vicinity of optical resonators that have been extensively used in surface-enhanced spectroscopy, both for luminescence and Raman scattering. As an example, Fig. 1(a) shows simulated local field enhancements in the vicinity of plasmonic and dielectric resonators, demonstrating how both types of materials can strongly enhance the excitation rate of emitters.

Regarding directivity, the induced multipolar modes in the nanoscale resonator, that is coherent with respect to the source dipole, will have specific phases and can, therefore, interfere constructively or destructively for specific outgoing wavevectors. This can provide the emission of the coupled emitter-resonator system

with a specific directivity similarly to classical antennas. This effect is crucial in optics because of the limited numerical aperture in detection. Therefore, matching the direction of emission and the collected wavevectors will optimize the detected luminescence signal.

Overall, all of these effects will lead to a modification of the detected luminescence signal for a quantum emitter in the vicinity of the nanoantenna. In a homogeneous environment (therefore, without the resonator), the photon flux collected in the far-field for a single emitter can be written as[38,39]

$$\Phi_0 = \kappa_0 \eta_0 \frac{\sigma I_0}{1 + I_0/I_{s_0}}, \tag{6}$$

with σ the excitation cross section of the quantum emitter (oriented along $\mathbf{u_p}$), κ_0 the collection efficiency of the experimental setup, $I_0 = |\mathbf{E_0}.\mathbf{u_p}|^2$ the excitation intensity for an incident field $\mathbf{E_0}$, and $I_{s_0} = \Gamma_0/\sigma$ the saturation intensity of the emitter. If the excitation intensity $I_0 \ll I_{s_0}$, then, Eq. (6) simplifies as $\kappa_0\eta_0\sigma I_0$ and the emitted flux is in the linear regime and equal to the rate of excitation multiplied by the quantum yield and corrected by the collection efficiency. If $I_0 \gg I_{s_0}$, then Φ_0 is independent of the excitation rate and equal to $\kappa_0\Gamma_{R_0}$. The photon flux in the saturation regime is simply the radiative rate corrected by κ_0 since the emitter is considered to always be in its excited state.

In most nanoantenna experiments, the excitation is kept low in order to consider the linear regime to be effective even when taking into account the local field enhancement. In that case, the increase in collected luminescence photon flux is given as[37,40]

$$\frac{\Phi}{\Phi_0} = \frac{\kappa}{\kappa_0}\frac{\eta}{\eta_0}\frac{I}{I_0} = \frac{\kappa}{\kappa_0}\frac{(I/I_0)(\Gamma_R/\Gamma_{R_0})}{1 - \eta_0 + \eta_0(\Gamma - \Gamma_{NR_0})/\Gamma_{R_0}}, \tag{7}$$

where κ is the collection efficiency of the setup with the resonator, Γ_R and $\eta = \Gamma_R/\Gamma$ the radiative rate and quantum yield of the emitter coupled to the resonator, I the excitation intensity in the near-field of the antenna, and $\Gamma_{NR_0} = \Gamma_0 - \Gamma_{R_0}$ the nonradiative decay rate of the emitter by itself. The reason why the more complex right part of the equation is often used when comparing experimental luminescence experiments to classical electrodynamics simulations is because Γ_R/Γ_{R_0} and $(\Gamma - \Gamma_{NR_0})/\Gamma_{R_0}$ are the relative decay rate changes, without and with the antenna, which are computed when considering a classical dipole without initial ohmic losses.

Overall, Eq. (7) demonstrates the combined effects of nanoantennas: local field enhancements to enhance the excitation rate; modified decay rates that modify the quantum yield; and modified collection efficiency thanks to emission directivity, that is, discussed in more detail in the next paragraph.

C. Controlling the emission directivity

The directivity of single emitters or scatterers in the far field is classically weak since the far-field radiation of all multipolar orders feature symmetric patterns. One of the objectives of optical antennas is to modify the electromagnetic coupling to quantum emitters in order to improve the collection of emitted photons for a given optical set-up with limited numerical aperture. The gain in directivity D_{dBi} is defined by the ratio between the radiated intensity in the direction of interest I and the total radiated power of the antenna P_{rad}: $D_{\mathrm{dBi}} = 10\log(4\pi I/P_{\mathrm{rad}})$.

The high potential of dielectric particles to collect light emission can be intuitively understood by the fact that, in optical waveguides, light is guided in high refractive index materials. The ability of dielectrics to collect light emission by electric dipoles was first studied in the context of a harmonic electric dipole in air above a dielectric substrate in 1977.[41,42] Recently, dielectric microspheres were used to enhance the excitation and to collect fluorescence signals.[43–46] The need for compactness and integrated devices motivated the development of efficient scatterers smaller than the wavelength; therefore, requiring a resonant interaction with light. Both plasmonic and high-index dielectric nanostructures can thus be considered.

To understand how an optically resonant scatterer strongly affects the emission pattern of a quantum emitter, and it is interesting to study the fundamental case of a single particle behaving as an induced electric dipole coupled with an emitting electric dipole.[47] The question is to predict the reflector or collector behavior of the particle coupled with the emitter. Strong directional emission is classically observed in the case where the source dipole is transversely coupled to the induced dipole. With α the polarizability of the resonant scatterer and d the distance between the emitter and induced dipole in the scatterer, it is possible to derive the relative phase ϕ between the source dipole and the induced dipole, as a function of the dimensionless parameter kd with $k = 2\pi/\lambda$. The relative phase, $\phi(kd) = \phi_\alpha + \phi_d(kd)$, contains two terms,[47]

$$\phi_\alpha = \mathrm{Arg}(\alpha),$$
$$\phi_d(kd) = \mathrm{Arg}(-e^{ikd}(1 - ikd - k^2d^2)).$$

The first term, ϕ_α, depends on the phase of the particle polarizability while the second term, $\phi_d(kd)$, depends on the emitter-to-particle distance d. The second term features two contributions: e^{ikd} describes the far field propagation, while the second term $1 - ikd - k^2d^2$ describes the near field coupling between the two dipoles. It can be demonstrated that the collector/reflector behavior can be simply predicted via the sign of sin (ϕ).[48] A collector behavior is associated with $\sin(\phi) > 0$ while a reflector behavior is observed when $\sin(\phi) < 0$. Let us first consider the case of a very small distance between the emitter and the particle, $kd \to 0$. In this case, $\phi_{\mathrm{d}} \to \pi$ and $\sin(\phi) \to -\sin[\arg(\alpha)] < 0$ since $\arg(\alpha) \in [0, \pi]$. We understand why the particle behaves like a collector when the emitter is very close to the particle. This property does not depend on the size and composition of the particle. When the emitter-to-particle distance increases, kd increases and ϕ decreases and reaches its minimum of $\phi \approx \frac{3\pi}{4}$ when $kd = \sqrt{2}$. In this case, the particle can either reflect or collect light depending on the phase of the particle polarizability. More precisely, the particle collects light if $\phi_\alpha < \pi/4$. We thus understand why the the size can play a crucial role since the phase due to the polarization ϕ_α experiences a strong shift around the dipolar resonance, from π to 0 for increasing wavelengths, the variation of phase being maximum around the resonance. Therefore, the collector behavior, corresponding to the condition $\phi_\alpha < \pi/4$, is observed for wavelengths

larger than the resonance wavelength. In other words, when considering a given emission wavelength, the condition $\phi_\alpha < \pi/4$ can be observed only for small particles (compared with the wavelength) which explains why the reflector element in Yagi-Uda antennas is composed of larger particles, while the collector element is composed of smaller particles.

Engineering nanoscale resonators capable of modifying the spontaneous decay rates and directivity of emitters as well as enhancing the optical near-field thus provides numerous degrees of freedom to produce optical nanoantennas. In the following paragraph, we focus more specifically on the specificities offered by high-index dielectric resonators to control emission directivity before discussing more generally the enhancement of luminescence signals with these nanostructures.

IV. DIRECTIONAL NANOANTENNAS

Optimizing emission directivity was successfully achieved with plasmonic systems, in particular, by downscaling the concept of Yagi-Uda antennas, initially developed at radiofrequencies.[49,50] Yagi-Uda antennas are composed of a reflector, a feed element and several collectors.[49] As discussed above, the reflector or collector behavior of particles depends on their shape and location with respect to the emitter.[47,48] The reflector is typically the largest element of this directive antenna, the feed element is made of a particle of intermediate size whose plasmon resonance matches the emission spectrum, while the collector is composed of several self similar smaller particles. The first experimental report involving a Yagi-Uda antenna composed of 5 elements (1 reflector, 1 feed and 3 collectors) was published in 2010 and demonstrated a gain in directivity as high as 6 dB using colloidal quantum dots as the emitting material.[51] A promising alternative consists in replacing the feed element by III-V nanowires, opening the route toward electrically driven optical Yagi-Uda antenna emitters.[52]

The main difference between plasmonic and dielectric directional antennas is that, in the case of plasmonic systems, only the induced electric dipole provides a nonnegligible radiated power, while for high-index nanostructures, all electric and magnetic multipolar modes can radiate. In 2011, it was shown that a single silicon particle behaves as an effective Huygens source and can switch the directivity of emission in the forward or backward scattering by simply tuning the emission frequency.[53] The concept of all-dielectric Yagi-Uda optical antennas was also introduced in the same study by coupling an emitter to 3 silicon particles, one forming the reflector and the other two forming the collector. It was also suggested to further increase the directivity by coupling additional particles in the collector element. This was done in 2012 by the same group by considering 4 self similar particles in the collector.[54] As discussed below, one of the main advantages of dielectric systems for directional emission comes from the interference between induced electric and magnetic dipoles in a single resonant scatterer.

A. Kerker conditions in the near-field

Extending the dipolar model used to derive Eq. (8) for particles featuring electric and magnetic dipolar resonances is equivalent to extending the so-called Kerker conditions to the near field. Let us briefly summarize that the Kerker conditions were originally established in the case of a magnetic scatterer illuminated from the far field[59] and were extended to the case of purely dielectric particles in 2011.[60,61] The first Kerker condition corresponds to a maximum of forward scattering associated with a vanishing backward scattering, while the second Kerker condition corresponds to a minimum of forward scattering. The observation of Kerker conditions in nonmagnetic particles is allowed by the excitation of electric and magnetic induced dipoles. While the conventional Kerker conditions are established when exciting a scatterer from the far field region, typically with a plane wave or a collimated beam, this concept can be extended to the near field by exciting a single high refractive index particle with an electric dipolar emitter. The key difference between the two configurations is the crucial role of the phase difference between the exciting electric dipole and the two dipoles induced in the scatterer. Compared to the previous case where only an electric dipole is induced in the resonator, the emitting electric dipole now also induces a magnetic dipole through its radiated magnetic field component. Optimizing the collecting behavior of the resonator corresponds to the 1st Kerker condition for a near field excitation: when the Poynting vector in the backward direction is minimized. Inversely, a strong reflector behavior is obtained when extending the 2nd Kerker condition to the near field in order to minimize forward scattering. These conditions are given as[55]

$$\begin{aligned} e^{-ikd} + \gamma_e\tilde{\alpha} &= \gamma_m\tilde{\beta}, \\ e^{ikd} + \gamma_e\tilde{\alpha} &\cong -\gamma_m\tilde{\beta}, \end{aligned} \tag{8}$$

where $\tilde{\alpha}$ and $\tilde{\beta}$ are the dimensionless electric and magnetic polarizabilities of the resonator, respectively; and γ_e and γ_m are dimensionless coupling parameters between the source electric dipole and the induced electric and magnetic dipoles, respectively.[55] The excitation of a magnetic dipole in the dielectric particle thus offers additional pathways to tailor the emission such as switching the directivity or increasing the gain in directivity. The coherent excitation of electric and magnetic induced dipoles in a scatterer can also be performed in plasmonics but this requires more complex shapes[62–64] or to couple different metallic nanowires.[65] Overall, coupling quantum emitters to multipolar classical scatterers allow for a more directive emission [Figs. 2(a) and 2(b)] than coupling them to a resonator that only features an induced electric dipole [Eq. (8)].

B. Practical implementations of directional antennas

At radiofrequencies, replacing metallic elements by dielectric resonators to produce antennas has been implemented for decades.[66,67] In this frequency range, materials with a wide range of dielectric permittivities can be implemented.[68–71] By tuning the real part of the dielectric constant, it is possible to change the quality factors of the resonances for applications where broadband or narrow-band responses are required. In particular, with broader Mie resonances, it is possible to achieve a spectral overlap between different multipolar modes. A high number of modes involved in the emission pattern allows for a fine tuning of the directivity. In that case, it is possible to switch the directivity from the forward

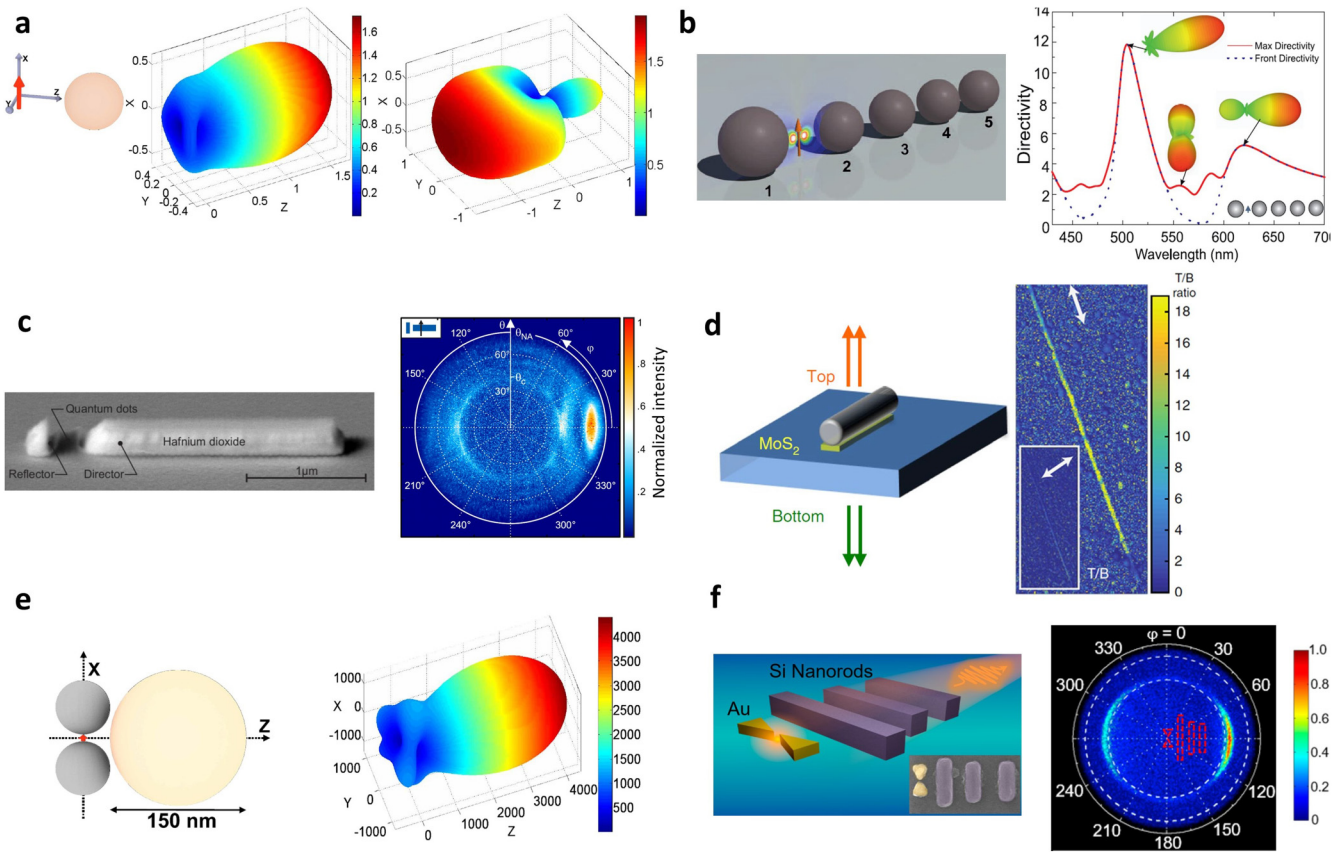

FIG. 2. Directional nanoantennas. (a) Near-field Kerker effect: theoretically calculated forward (left) and backward (right) light emission of an electric dipole emitter transversely coupled with a 85 nm radius GaP nanosphere and emitting at $\lambda = 550$ nm. Adapted with permission from Rolly *et al.*, Opt. Express **20**, 20376–20386 (2012). Copyright 2012 Optical Society of America. (b) All-dielectric Yagi-Uda antenna: sketch of the considered structure and simulated directivity as a function of the wavelength. Adapted with permission from Krasnok *et al.*, Opt. Express **20**, 20599–20604 (2012). Copyright 2012 Optical Society of America. (c) Dielectric hafnium dioxide-based antenna: electron microscopy image (top) and experimentally measured emission pattern from quantum dots positioned in the gap (bottom). Adapted with permission from Peter *et al.*, Nano Lett. **17**, 4178–4183 (2017). Copyright 2017 American Chemical society. (d) Directional emission from monolayer MoS_2 using a silicon nanorod: sketch of the sample (left) and 2D map of the ratio between top and bottom emission directions (right). Adapted with permission from Cihan *et al.*, Nat. Photonics **12**, 284 (2018). Copyright 2018 Nature Publishing Group. (e) Hybrid plasmon-dielectric antenna: a silver dimer is coupled to a GaP nanosphere (scheme on the left) to ensure both enhanced and directional emission (theoretical emission pattern on the right). Adapted with permission from Rolly *et al.*, Opt. Express **20**, 20376–20386 (2012). Copyright 2012 Optical Society of America. (f) Hybrid structure comprising a gold bowtie antenna and a silicon-based Yagi Uda antenna: scheme and electron microscopy image (left) and measured directional emission using the nonlinear luminescence of gold (right). Adapted with permission from Ho *et al.*, ACS Nano **12**, 86168624 (2018). Copyright 2018 American Chemical society.

direction to the backward direction by simply modifying the emission frequency. For instance, the coupling between the emission dipole and higher order modes of the dielectric scatterer can be achieved by considering a notch in the dielectric antenna. Placing the emitter inside the notch offers highly directive antennas.[71]

A first experimental realization and characterization of an all-dielectric directive antenna in the visible spectrum was reported in 2017.[56] The antenna was composed of a reflector and a collector made of hafnium dioxide and the light source was provided by quantum dots deposited into the feed gap between director and reflector [see Fig. 2(c)].

An interesting aspect of all-dielectric antennas is their ability to optimize emission directivity of 2D transition metal dichalcogenides materials such as WSe_2, $MoSe_2$, WS_2, and MoS_2. 2D materials benefit from intense efforts since they combine many essential features for opto-electronics applications. In particular, they are cost effective, extremely thin (atomic scale) and their flatness makes them ideal candidates for developing integrated photon sources.[72] The coupling with optical antennas is particularly interesting since it will redirect the emission to a direction normal to the surface.[73] As discussed in Eq. (8), the distance between the emitter and the antenna is crucial to control the emission directivity, this is why an atomically flat solid-state light source is particularly well-suited to control the emitter-to-antenna distance at the nanoscale. A major innovation was presented in 2018 by redirecting the photon emission of an atomically thin MoS_2 layer with a silicon nanowire exhibiting electric and

magnetic Mie resonances.[57] A forward-to-backward ratio of 20 was reported at the emission wavelength of 680 nm. This study nicely combines the photoluminescence properties of 2D materials with the scattering properties of silicon nanorods[74] to redirect the fluorescence emission in a direction normal to the plane. Interestingly, 2D dichalcogenides materials can be integrated with dielectric metasurfaces,[75] and their interaction with dielectric antennas should reach strong-coupling regimes.[73]

It is interesting to note that plasmonic and Mie resonators can be judiciously combined in hybrid metal-dielectric antennas[76–79] [see Figs. 2(d) and 2(e)]. Indeed, Mie resonators feature high extinction cross sections when excited from the far field and reciprocally, they can provide high directivity when excited from the near field; while plasmonic systems offer strong local fields to enhance the luminescence signal.[58,80–82] As shown in the examples of Figs. 2(d) and 2(e), the plasmonic nanoparticles are generally coupled longitudinally to each other to provide a nanoscale hot-spot, but are coupled transversely to the dielectric resonators to maximize the directivity as discussed in Eq. (8).

V. MANIPULATING LUMINESCENCE FROM ELECTRIC EMITTERS

A. Optimizing excitation and emission rates

Because of reciprocity, a strong enhancement of the local electric field at a given position in a nanoantenna will lead to a similar increase of the radiative decay rate from an electric dipolar emitter introduced at the same location.[19,36,37,83] This is why dimers of gold nanoparticles separated by a nanoscale gap, as discussed in Fig. 1, have been extensively used to enhance the excitation and spontaneous decay rates of single fluorescent molecules.[84–86] Similarly, dimers of thin silicon particles featuring a nanoscale gap were proposed as early as 2007 to enhance locally the intensity of the electric field.[87] While thin silicon particles mainly lead to an enhancement of the electric field in the surrounding medium, thicker nanostructures like spheres exhibit a completely different distribution of the electromagnetic near fields with strong amplitudes inside the resonators and enhanced magnetic fields, as shown in Fig. 1. Experimentally, enhanced electric and magnetic fields in the nanogap of silicon dimers were probed with near-field scanning optical microscopy.[88]

One of the difficulties in analyzing the enhancement of spontaneous emission by optical nanoantennas is the ability of introducing fluorescent emitters specifically in the near-field of nanoscale resonators. The first experiments describing fluorescence enhancement in the vicinity of silicon nanowires or disk dimers were performed using an homogeneous layer of fluorescent molecules at the diffraction limit, introducing spatial averaging.[95,96] Alternatively, two approaches can be implemented as described in Figs. 3(a) and 3(b): the use of freely diffusing molecules[89] and scanning-probe microscopy.[90] The first technique allows an estimation of the fluorescence enhancement per molecule as a function of the gap size and demonstrates nicely that silicon nanodisk dimers lead to a gain in brightness larger than two orders of magnitude, similarly to what is observed in gold dimers [Fig. 3(a)]. The advantage of scanning-probe microscopy is the ability to measure fluorescence intensities and lifetimes of the emitter as a function of the distance to the antenna with nanoscale accuracy [Fig. 3(b)].

The coupling between fluorescent emitters and dielectric resonators can be engineered by tuning the materials that are used to produce the antenna.[97] In particular, GaP provides an efficient platform to enhance both second harmonic generation (SHG) and fluorescence signals.[98] Furthermore, the coupling efficiency can be actively controlled by tuning the resonance properties of the dielectric resonators, for instance, by using liquid crystal layer [Fig. 3(c)].[91] In this case, the resonators are organized in a 2D resonant metasurface to gain extra degrees of freedom in designing the optical response of the coupled system. Several other implementations of the coupling between emitters and dielectric metasurfaces were demonstrated, in particular, to associate a gain in photoluminescence intensity and emission directivity.[94,99,100]

An alternative strategy to optimize the coupling between luminescent solid-state systems and dielectric nanoantennas is to embed dipolar electric emitters directly inside the resonators where the electric near-fields and Purcell factors can be maximum.[101,102] Figures 3(d)–3(f) provide recent experimental realizations using either Ge(Si) quantum dots in silicon nanodisks,[92] hybrid perovskite nanoparticles (which act as both the resonator and emitting material),[93] and InAs quantum dots in GaAs resonant metasurfaces.[103]

All of these experimental demonstrations clearly highlight the ability of high-index nanoantennas to enhance light absorption and emission by solid-state systems. The extension of these processes to the near-infrared range (where emitters are usually poor in terms of quantum yields and/or excitation cross sections) as well as the integration of these resonators in optoelectronic systems are certainly two of the main perspectives of this scientific field.

B. Inhibition of spontaneous emission

One of the main properties of high-index dielectric nanoantennas is their ability to modify the radiative decay rate of emitters without introducing nonradiative decay channels (as long as the considered wavelength is close or higher than the material bandgap). This opens new degrees of freedom in manipulating light-matter interactions, in particular, by inhibiting spontaneous emission. Indeed, in classical electrodynamics, if the induced multipoles in the resonator interfere destructively with the source electric dipole of the emitter, then the power radiated in the far-field will be reduced. According to Eqs. (4) and (5), this will lead to a reduction of the radiative decay rate. While such a phenomenon is possible in plasmonic systems,[104] it will be masked by the nonradiative decay channels introduced by lossy metals. This is no longer the case with high-index dielectrics: reduced radiative decay rates will lead to an increased luminescence lifetime even in close proximity to the antenna. This is directly observed in Fig. 3(b) when considering an antenna, that is, either in- or out-of-phase with respect to the fluorescent emitters: an in-phase antenna leads to an increased total decay rate, while an out-of-phase resonator leads to an inhibition of spontaneous emission with a similar order of magnitude.[90] This is expected from Eq. (8), which shows how a wavelength mismatch will modify the phase ϕ_α of the induced dipole in the resonator.

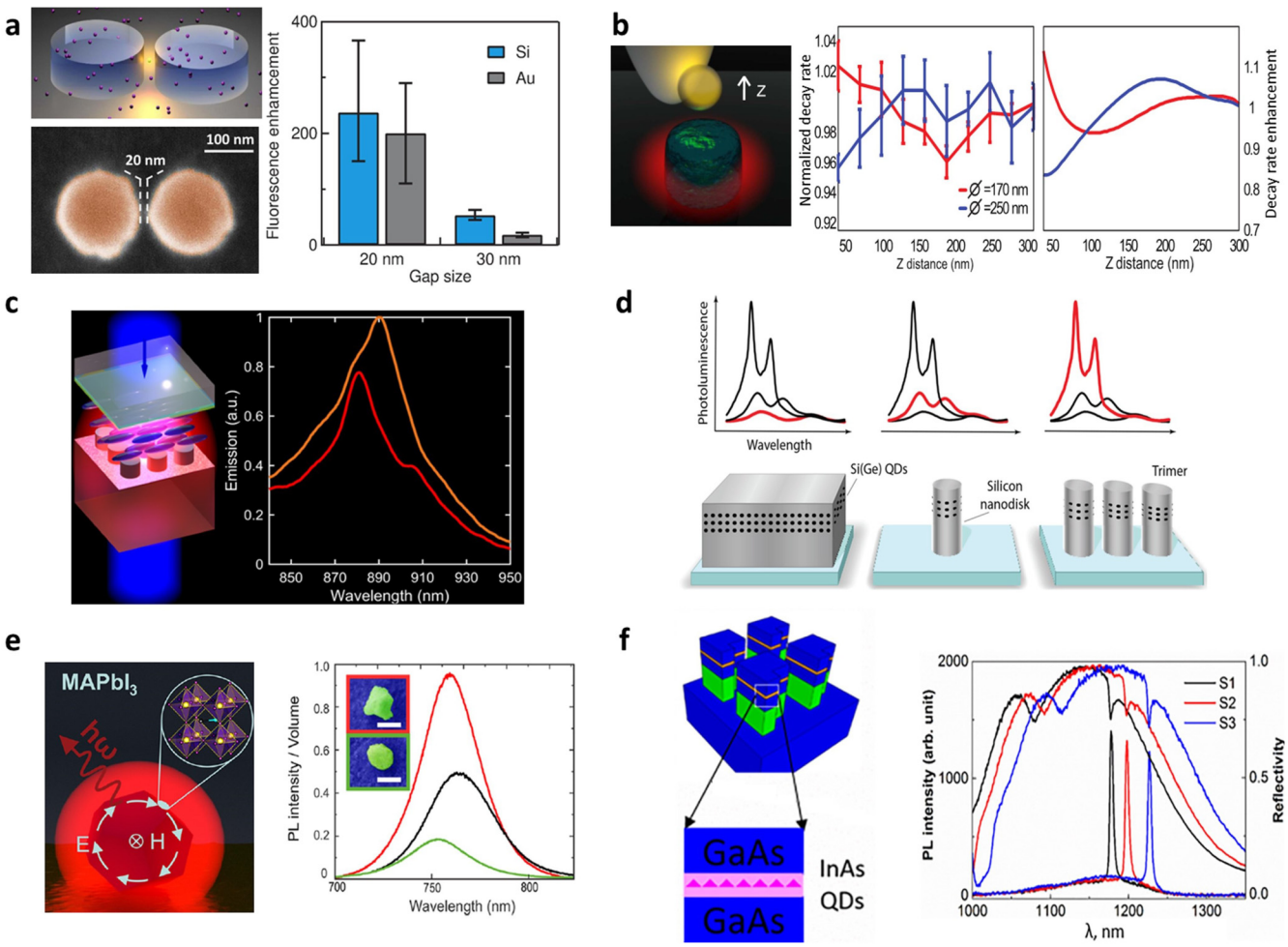

FIG. 3. Spontaneous electric emission in the near-field of dielectric nanoantennas. (a) Silicon nanogap antenna used to enhance fluorescence from freely diffusing molecules: scheme of the sample and electron microscopy image (left) and estimated fluorescence enhancement values as a function of the gap length for silicon and gold nanodisk dimers (right). Adapted with permission from Regmi *et al.*, Nano Lett. **16**, 5143–5151 (2016). Copyright 2016 American Chemical Society. (b) Enhancement and inhibition of spontaneous emission from a fluorescent nanosphere in the near field of silicon disks as a function of their relative distance *z* (varied in scanning probe microscopy): scheme of the experiment with the fluorescent sphere grafted at the apex of a tapered optical fiber (left); measured (centre) and simulated (right) decay rate changes as a function of *z* when the antenna is resonant (blue) or out-of-resonance (red) with the emitters. Adapted with permission from ref Bouchet *et al.*, Phys. Rev. Appl. **6**, 064016 (2016). Copyright 2016 American Institute of Physics. (c) Active control of spontaneous emission with a resonant silicon metasurface associated with a liquid-crystal layer: scheme of the sample (left) and measured modification of the emission (right). Adapted with permission from Bohn *et al.*, Nano Lett. **18**, 3461–3465 (2018). Copyright 2018 American Chemical Society. (d) Enhancement of luminescence from Si(Ge) quantum dots embedded in silicon layers (left), nanodisks (centre) and nanodisk trimers (right). Adapted with permission from Rutckaia *et al.*, Nano Lett. **17**, 6886–6892 (2017). Copyright 2017 American Chemical Society. (e) Enhanced luminescence from hybrid perovskite nanoparticles acting both as the emitting material and as a Mie resonator. Adapted with permission from Tiguntseva *et al.*, Nano Lett. **18**, 1185–1190 (2018). Copyright 2018 American Chemical Society. (f) Control of luminescence from InAs quantum dots embedded in GaAs resonant metasurfaces: scheme of the sample (left) and measured photoluminescence and reflectivity spectra as a function of the metasurface geometry (right). Adapted with permission from Vaskin *et al.*, ACS Photonics **5**, 1359–1364 (2018). Copyright 2018 American Chemical Society.

However, one can observe that the measured decay rate changes in Fig. 3(b) remain weak because a single Si nanodisk is an inefficient antenna (and because the size of the fluorescent emitter—a 100 nm diameter sphere—leads to spatial averaging of the coupling process). As discussed in Figs. 1 and 3(a), particle dimers are more efficient systems to tune the spontaneous emission properties of luminescent systems. Simulations performed with dimers of silicon nanospheres indicated that an inhibition of spontaneous emission by more than one order of magnitude is possible for transversely coupled emitters.[105] However, the experimental demonstration of strongly inhibited spontaneous emission at room temperature using a dielectric antenna has not yet been realized while it has been observed with atomic systems[106] and in the solid-state at cryogenic temperatures.[5–9] While reciprocity

associates an inhibited radiative decay rate to an inhibited excitation rate,[19,83] it should be possible to exploit large Stokes shifts in order to associate enhanced excitation and enhanced energy storage in electronic excited states, opening new strategies to harvest light in the solid state.

VI. ENHANCING SPONTANEOUS EMISSION MEDIATED BY MAGNETIC TRANSITION DIPOLES

A. Favoring magnetic emission

As shown in Fig. 1, an important property of dielectric antennas is their ability to feature both electric and magnetic multipolar resonances, allowing them to manipulate spontaneous decay processes mediated by both electric and magnetic transition dipoles. Magnetic dipolar transitions in solid-state materials were first considered to probe artificial magnetism in optical metamaterials.[111–113] In 2010, Zia and co-workers demonstrated that the emission mediated by magnetic transition dipoles in trivalent lanthanide ions could be tuned by modifying the electromagnetic environment in the vicinity of a planar mirror.[114,115] Indeed, the high symmetry of 4*f* electronic wavefunctions in lanthanide ions forbids electric dipolar transitions and renders them of a similar amplitude to their magnetic counterpart.[18,27] In particular, Eu^{3+} emitters feature both a $^5D_0 \rightarrow ^7F_2$ transition around 610 nm mediated by an electric transition dipole (ED, which was used in seminal experiments devoted to modified spontaneous emission of electric emitters in front of a mirror)[116,117] and a $^5D_0 \rightarrow ^7F_1$ transition around 588 nm, that is, associated to a magnetic transition dipole (MD). These competitive transitions, which originate from the same excited state, allow an analysis of the relative electric and magnetic local density of radiative electromagnetic states from intensity measurements only.[34,115,118–121]

One difficulty in exploiting dielectric antennas to control spontaneous emission mediated by magnetic dipolar transitions is that the area of the resonator where the magnetic field is the highest is typically its centre [see Fig. 1(a)]. Furthermore, because the ED and MD transitions of lanthanide ions are competitive, a resonator should only enhance the magnetic emission and not the electric emission at a given position. For instance, as shown in Fig. 1(b), the gap of a dimer antenna enhances the decay rate of a magnetic emitter but enhances the electric counterpart more efficiently. An interesting alternative design to circumvent this issue was proposed by hollowing out a silicon nanodisk: such structures yield strong magnetic near-field inside the disk and enhance the electric near-field on its edges.[107,122–125]

Figure 4(a) presents an experimental analysis of the coupling between a hollow silicon nanodisk (milled at the apex of a scanning-probe tip) and a Eu^{3+} doped oxide nanoparticle using near-field microscopy.[107] By measuring independently the photoluminescence intensities of the $^5D_0 \rightarrow ^7F_1$ MD (590 nm) and $^5D_0 \rightarrow ^7F_2$ ED (610 nm) transitions, it is possible to map, with nanoscale precision, the relative magnetic and electric local

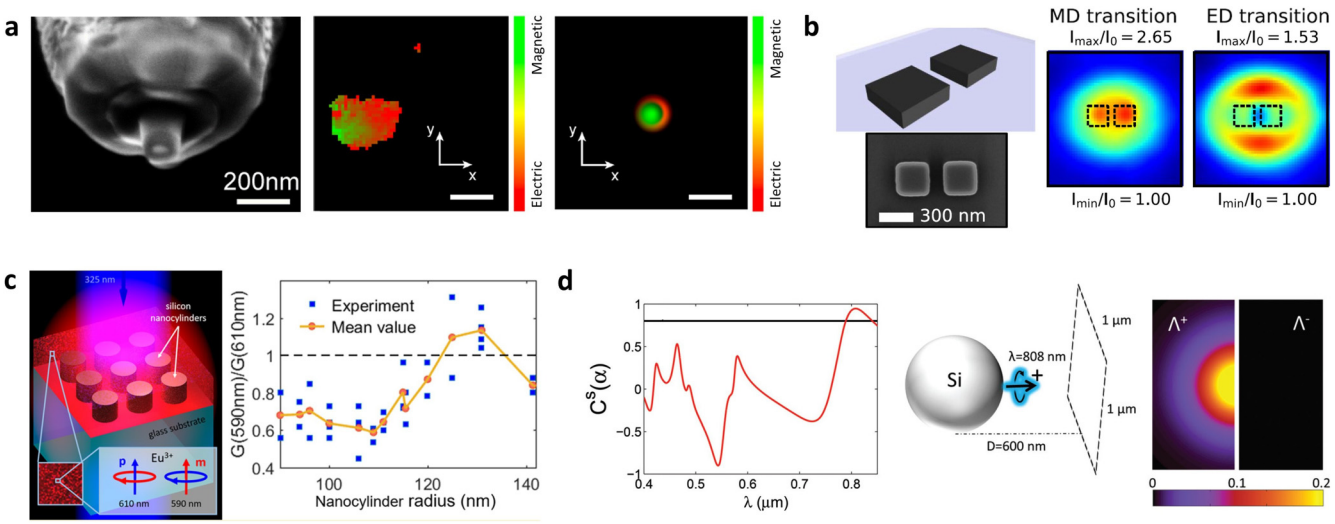

FIG. 4. Dielectric antennas to manipulate magnetic and chiral emission. (a) Hollow cylindrical antenna made of silicon to enhance electric or magnetic emission from a europium-doped oxide nanoparticle: electron microscopy image of the silicon antenna milled on a scanning-probe tip by focused ion beam (left), measured nanoscale map of the relative magnetic and electric local density of radiative optical states (center) compared to simulated magnetic and electric local field enhancements (right). Adapted with permission from Sanz-Paz *et al.*, Nano Lett. **18**, 3481–3487 (2018). Copyright 2018 American Chemical Society. (b) Silicon nanodimer to modify the emission of europium cations: scheme and electron microscopy image of the sample (left) and magnetic (center) and electric (right) luminescence maps. Adapted with permission from Wiecha *et al.*, Appl. Opt. **58**, 1682–1690 (2019). Copyright 2019 Optical Society of America. (c) Silicon metasurface to modify the relative magnetic/electric emission of europium: scheme of the sample (left) and measured emission ratio as a function of the metasurface geometry (right). Adapted with permission from Vaskin *et al.*, Nano Lett. **19**, 1015–1022 (2019). Copyright 2019 American Chemical Society. (d) Theoretical modification of the chirality of the light emitted by a chiral emitter in the near-field of a 100 nm radius silicon sphere: spectral dependence (left) and perfectly chiral emission at 808 nm (right). Adapted with permission from Zambrana-Puyalto and Bonod, Nanoscale **8**, 10441–10452 (2016). Copyright 2016 Royal Society of Chemistry.

densities of radiative states around the antenna that feature well-separated areas in good agreement with simulated near-field intensities [Fig. 4(a)].

Figures 4(b) and 4(c) describe two other experimental realizations of the coupling between Eu^{3+} emitters and silicon-based nanoantennas and metasurfaces, clearly showing the potential of dielectric resonators to manipulate magnetic emission processes.[108,109] However, in all of these experimental demonstrations, the gain in magnetic over electric emission remains weak (below 10) because of the technical complexity in positioning specifically the emitters at a chosen position of the resonator without spatial averaging. One solution is to adapt the geometry of the dielectric antenna in order to feature magnetic fields that are more easily accessible than the center of a hollow silicon nanodisk, as recently proposed theoretically using genetically designed resonators.[126] Another solution would be to adapt the nanofabrication methods in order to fully exploit the high magnetic density of states in the center of resonators. Overall, the search for a bright purely magnetic nanoscale light source in the solid state is still ongoing. While the enhancement of spontaneous emission associated to magnetic transition dipoles may appear primarily as a fundamental analysis of spectroscopic selection rules, it opens several perspectives in developing spectrally switchable light sources[127] but also in the structural analysis of active materials since magnetic emission processes are strongly sensitive to the local symmetry of electronic wavefunctions.[18,128]

B. Controlling the chirality of light emission

In the previous sections, we discussed the control of electric and magnetic spontaneous emission or the optimization of one decay process over the other. Interestingly, it is possible to design dielectric resonators that feature partially superimposed electric and magnetic resonances in order to enhance processes mediated by both electric and magnetic dipolar transitions, as well as mixed electric-magnetic polarizabilities, such as optical chirality.[129] For instance, this provides dielectric resonators with the ability to enhance circular dichroism or enantioselective optical sensing.[130–134]

Another approach to control the chirality of light-matter interactions using dielectric resonators arises when considering chiral spontaneous emission. Chiral emitters feature both electric and magnetic transition dipoles, with $\mathbf{p}$ being of real amplitude and $\mathbf{m}$ of complex amplitude.[135,136] The light emitted in the far field by the ensemble "chiral emitter/spherical dielectric particle" can be analyzed in a $+1$ and -1 helicity basis. A scattered field exhibits high chiral properties if it can be expanded in one of the $+1$ or -1 helicity components only. As electric or magnetic dipolar modes are split 50%/50% on the $+1$ and -1 helicity components basis then, a resonator featuring both electric and magnetic modes provides the required degrees of freedom to manipulate the helicity of light emission as demonstrated in Fig. 4(d) when introducing a chiral emitter in the near-field of a silicon sphere. Emission of the chiral emitter is seen to be mostly in the $+1$ helicity (left panel) at $\lambda = 808$ nm. A similar theoretical calculation with a gold nanosphere, featuring mostly an electric dipolar resonance, indicates an equal contribution between the two helicities.[110] When plotting the degree of helicity with respect to the wavelength, we observe that the silicon particle can either increase or reduce the chirality of light emission in given wavelength ranges. We can also observe that the helicity of light emission can be preserved at two given frequencies, i.e. when the degree of helicity of the scattered light is equal to the degree of helicity of the emitter itself. One of these frequencies corresponds to the case where all electric and magnetic Mie components in the resonator are equal for each multipolar order, confirming that dual scatterers, featuring both electric and magnetic modes, preserve the helicity of light.[137]

One difficulty in demonstrating these phenomena experimentally comes from the complexity in producing efficient chiral emitters. However, recent practical demonstrations using quantum dots in high magnetic fields (using the Zeeman effect),[138] transition metal dichalcogenides,[139,140] or organic dyes[141,142] open several possibilities to study experimentally the ability of high-index resonators to control the helicity of spontaneous emission. Producing efficient chiral emitters at room temperature opens numerous perspectives to produce nonreciprocal directional light sources or to encode the spin state of a solid-state emitter in an optical signal.[138–140]

VII. CONCLUSION and PERSPECTIVES

This perspective highlights the numerous degrees of freedom offered by dielectric resonators to manipulate spontaneous emission from the solid-state at room temperature. In particular, the weak ohmic losses and strong electromagnetic fields inside dielectric resonators provide electric and magnetic multipolar modes that influence electric or magnetic emitters by tuning mainly radiative decay channels. This allows not only the enhancement of the excitation and emission rates from luminescent sources (similarly to plasmonic antennas) but also a complex engineering of the emission directivity (using the far-field interference of several induced modes in the resonator), a possible inhibition of spontaneous emission as well as a control of emission helicity.

However, gaining these degrees of freedom in manipulating spontaneous emission also renders the optimized design of dielectric resonators particularly complex. A full electrodynamic understanding of the modal decomposition of the induced modes in complex shaped nanostructures is, therefore, required but, more generally, the antenna designs will benefit from the latest advances in numerical optimization such as evolutionary algorithms,[126,143] inverse design,[144] and deep learning.[145] These strategies will be particularly important when envisioning complex light-matter processes such as light-harvesting (requiring an optimized excitation but an inhibited emission) or magnetic emission (which should be associated to a minimized electric emission). While preliminary studies described in Figs. 3(b) and 4 demonstrate the potential of dielectric resonators, the modest decay rate modifications reported until now clearly evidence a need in optimizing both the antenna designs and coupling efficiencies. There are, therefore, several experimental milestones that are, in our opinion, still to be achieved. In particular, advances in nanofabrication strategies will be required to reach orders of magnitude enhancements of magnetic emission or of inhibited emission as was reported for the enhancement of electric emission.[89]

Regarding the optimization of the photoluminescence from electric emitters by optimizing the directivity as well as the excitation and emission rates, recent reports have already demonstrated

high efficiencies (Figs. 2 and 3). It is, however, essential to validate these resonator designs by integrating them efficiently in optoelectronic devices, in particular, to obtain electrically excited optimized light sources. In that sense, high-index dielectric nanoantennas will benefit from the current advances in material technology for both the emitters and resonant nanostructures. While silicon has been extensively investigated, other semiconductors will be of interest, in particular, to introduce emitters at controlled positions inside the resonators [Figs. 3(d)–3(f)]. The external active control of antenna properties[91] will provide further complexity and tunability in the design of all-dielectric resonators.

In that sense, transition metal dichalcogenides are particularly interesting for optoelectronic integration but also to reach strong-coupling regimes[73] or to study chiral luminescence properties.[139,140] In particular, reaching a 100% degree of circular polarization, associated to directional coupling in an integrated photonic device, is an essential result in order to exploit the spin-orbit coupling of light in practical applications. Furthermore, the ability to produce dielectric resonators directly from transition metal dichalcogenides[146] is an exciting possibility to create fully integrated nanophotonic platforms combining active emission, optical resonances, and nonlinear responses.

While this perspective was focused essentially on spontaneous emission, an important application of dielectric resonators coupled to active materials is the manipulation of stimulated emission through the design of novel nanolasers. Nanolasers were first investigated in plasmonics where a single particle[147] or an array of particles[148–151] coupled with a gain material forms a cavity in which stimulated emission can occur. The main interest of dielectric resonators is that the gain material can be introduced inside the dielectric cavity where the Purcell factor is maximized[101] or the gain material itself can be used to form the resonant laser cavity. Interestingly, lasing from a single chemically-synthesized halide perovskite $CsPbBr_3$ nanocube was recently demonstrated, the considered material acting as both gain medium and Mie resonant cavity.[152] This bottom-up approach is promising to develop laser nanocavities driven by low order Mie resonances at large scales. An alternative approach consists in properly engineering the coupling between induced modes in 2D arrays of dielectric resonators (exploiting, for instance, bound states in the continuum),[153–155] in order to develop low threshold lasers based on high quality factor resonances.[156,157] These are crucial steps in the quest for fully integrated nanolasers, for which achieving continuous-wave light pumping or electrical excitation will be essential milestones.

Overall, the optimized coupling between all-dielectric nanoantennas and solid-state emitters, through a combined effort in resonator design and nanofabrication strategies, is expected to provide compact, integrated and highly efficient light sources, in terms of brightness, decay rates, and directivity.

ACKNOWLEDGMENTS

S.B. acknowledges support from LabEx WIFI (Laboratory of Excellence within the French Program "Investments for the Future") under Reference Nos. ANR-10-LABX-24 and ANR-10-IDEX-0001-02 PSL*. The authors thank Francesca Legittimo for performing some of the simulations of Fig. 1.

REFERENCES

[1]A. B. Evlyukhin, C. Reinhardt, A. Seidel, B. S. Luk'yanchuk, and B. N. Chichkov, "Optical response features of Si-nanoparticle arrays," Phys. Rev. B **82**, 045404 (2010).
[2]A. García-Etxarri, R. Gómez-Medina, L. S. Froufe-Pérez, C. López, L. Chantada, F. Scheffold, J. Aizpurua, M. Nieto-Vesperinas, and J. J. Sáenz, "Strong magnetic response of submicron silicon particles in the infrared," Opt. Express **19**, 4815–4826 (2011).
[3]A. B. Evlyukhin, S. M. Novikov, U. Zywietz, R. L. Eriksen, C. Reinhardt, S. I. Bozhevolnyi, and B. N. Chichkov, "Demonstration of magnetic dipole resonances of dielectric nanospheres in the visible region," Nano Lett. **12**, 3749–3755 (2012).
[4]A. I. Kuznetsov, A. E. Miroshnichenko, Y. H. Fu, J. Zhang, and B. Lukyanchuk, "Magnetic light," Sci. Rep. **2**, 492 (2012).
[5]E. Yablonovitch, "Inhibited spontaneous emission in solid-state physics and electronics," Phys. Rev. Lett. **58**, 2059 (1987).
[6]M. Bayer, T. L. Reinecke, F. Weidner, A. Larionov, A. McDonald, and A. Forchel, "Inhibition and enhancement of the spontaneous emission of quantum dots in structured microresonators," Phys. Rev. Lett. **86**, 3168–3171 (2001).
[7]M. Fujita, S. Takahashi, Y. Tanaka, T. Asano, and S. Noda, "Simultaneous inhibition and redistribution of spontaneous light emission in photonic crystals," Science **308**, 1296–1298 (2005).
[8]S. Noda, M. Fujita, and T. Asano, "Spontaneous-emission control by photonic crystals and nanocavities," Nat. Photonics **1**, 449–458 (2007).
[9]J. Bleuse, J. Claudon, M. Creasey, N. S. Malik, J. M. Gerard, I. Maksymov, J. P. Hugonin, and P. Lalanne, "Inhibition, enhancement, and control of spontaneous emission in photonic nanowires," Phys. Rev. Lett. **106**, 103601 (2011).
[10]M. Agio, "Optical antennas as nanoscale resonators," Nanoscale **4**, 692–706 (2012).
[11]A. F. Koenderink, "Single-photon nanoantennas," ACS Photonics **4**, 710–722 (2017).
[12]F. Marquier, C. Sauvan, and J.-J. Greffet, "Revisiting quantum optics with surface plasmons and plasmonic resonators," ACS Photonics **4**, 2091-2101 (2017).
[13]S. Albaladejo, R. Gómez-Medina, L. Froufe-Pérez, H. Marinchio, R. Carminati, J. Torrado, G. Armelles, A. García-Martín, and J. J. Saénz, "Radiative corrections to the polarizability tensor of an electrically small anisotropic dielectric particle," Opt. Express **18**, 3556–3567 (2010).
[14]M. Meier and A. Wokaun, "Enhanced fields on large metal particles: Dynamic depolarization," Opt. Lett. **8**, 581–583 (1983).
[15]A. Moroz, "Depolarization field of spheroidal particles," J. Opt. Soc. Am. B **26**, 517–527 (2009).
[16]R. Colom, A. Devilez, S. Enoch, B. Stout, and N. Bonod, "Polarizability expressions for predicting resonances in plasmonic and Mie scatterers," Phys. Rev. A **95**, 063833 (2017).
[17]A. Devilez, X. Zambrana-Puyalto, B. Stout, and N. Bonod, "Mimicking localized surface plasmons with dielectric particles," Phys. Rev. B **92**, 241412 (2015).
[18]C. M. Dodson and R. Zia, "Magnetic dipole and electric quadrupole transitions in the trivalent lanthanide series: Calculated emission rates and oscillator strengths," Phys. Rev. B **86**, 125102 (2012).
[19]L. Novotny and N. van Hulst, "Antennas for light," Nat. Photonics **5**, 83–90 (2011).
[20]A. F. Koenderink, "Single-photon nanoantennas," ACS Photonics **4**, 710–722 (2017).
[21]J.-J. Greffet, M. Laroche, and F. Marquier, "Impedance of a nanoantenna and a single quantum emitter," Phys. Rev. Lett. **105**, 117701 (2010).
[22]L. Novotny, "From near-field optics to optical antennas," Phys. Today. **64**, 47–52 (2011).
[23]D. Bouchet and R. Carminati, "Quantum dipole emitters in structured environments: A scattering approach: tutorial," J. Opt. Soc. Am. A **36**, 186–195 (2019).
[24]L. Novotny and B. Hecht, *Principles of Nano-Optics* (Cambridge University Press, 2006).

[25]R. Carminati, J. J. Greffet, C. Henkel, and J. M. Vigoureux, "Radiative and non-radiative decay of a single molecule close to a metallic nanoparticle," Opt. Commun. **261**, 368–375 (2006).
[26]A. E. Krasnok, A. P. Slobozhanyuk, C. R. Simovski, S. A. Tretyakov, A. N. Poddubny, A. E. Miroshnichenko, Y. S. Kivshar, and P. A. Belov, "An antenna model for the Purcell effect," Sci. Rep. **5**, 12956 (2015).
[27]C. M. Dodson, J. A. Kurvits, D. Li, M. Jiang, and R. Zia, "Magnetic dipole emission of Dy^{3+}:Y_2O_3 and Tm^{3+}:Y_2O_3 at near-infrared wavelengths," Opt. Mater. Express **4**, 2441–2450 (2014).
[28]J. R. Zurita-Sánchez and L. Novotny, "Multipolar interband absorption in a semiconductor quantum dot. I. Electric quadrupole enhancement," J. Opt. Soc. Am. B **19**, 1355–1362 (2002).
[29]J. R. Zurita-Sánchez and L. Novotny, "Multipolar interband absorption in a semiconductor quantum dot. II. Magnetic dipole enhancement," J. Opt. Soc. Am. B **19**, 2722–2726 (2002).
[30]M. L. Andersen, S. Stobbe, A. S. Sørensen, and P. Lodahl, "Strongly modified plasmon–matter interaction with mesoscopic quantum emitters," Nat. Phys. **7**, 215 (2011).
[31]K. Joulain, R. Carminati, J.-P. Mulet, and J.-J. Greffet, "Definition and measurement of the local density of electromagnetic states close to an interface," Phys. Rev. B **68**, 245405 (2003).
[32]B. Rolly, B. Bebey, S. Bidault, B. Stout, and N. Bonod, "Promoting magnetic dipolar transition in trivalent lanthanide ions with lossless Mie resonances," Phys. Rev. B **85**, 245432 (2012).
[33]M. K. Schmidt, R. Esteban, J. Sáenz, I. Suárez-Lacalle, S. Mackowski, and J. Aizpurua, "Dielectric antennas—A suitable platform for controlling magnetic dipolar emission," Opt. Express **20**, 13636–13650 (2012).
[34]D. G. Baranov, R. S. Savelev, S. V. Li, A. E. Krasnok, and A. Alù, "Modifying magnetic dipole spontaneous emission with nanophotonic structures," Laser. Photon. Rev. **11**, 1600268 (2017).
[35]P. R. Wiecha, A. Arbouet, A. Cuche, V. Paillard, and C. Girard, "Decay rate of magnetic dipoles near nonmagnetic nanostructures," Phys. Rev. B **97**, 085411 (2018).
[36]R. Carminati, M. Nieto-Vesperinas, and J.-J. Greffet, "Reciprocity of evanescent electromagnetic waves," J. Opt. Soc. Am. A **15**, 706–712 (1998).
[37]P. Bharadwaj and L. Novotny, "Spectral dependence of single molecule fluorescence enhancement," Opt. Express **15**, 14266–14274 (2007).
[38]J. Wenger, "Fluorescence enhancement factors on optical antennas: Enlarging the experimental values without changing the antenna design," Int. J. Opt. **2012**, 828121 (2012).
[39]J. Wenger, D. Gérard, J. Dintinger, O. Mahboub, N. Bonod, E. Popov, T. W. Ebbesen, and H. Rigneault, "Emission and excitation contributions to enhanced single molecule fluorescence by gold nanometric apertures," Opt. Express **16**, 3008–3020 (2008).
[40]S. Bidault, A. Devilez, V. Maillard, L. Lermusiaux, J. M. Guigner, N. Bonod, and J. Wenger, "Picosecond lifetimes with high quantum yields from single-photon-emitting colloidal nanostructures at room temperature," ACS Nano **10**, 4806–4815 (2016).
[41]W. Lukosz and R. Kunz, "Light emission by magnetic and electric dipoles close to a plane interface. I. Total radiated power," J. Opt. Soc. Am. **67**, 1607–1615 (1977).
[42]W. Lukosz and R. Kunz, "Light emission by magnetic and electric dipoles close to a plane dielectric interface. II. radiation patterns of perpendicular oriented dipoles," J. Opt. Soc. Am. A **67**, 1615–1619 (1977).
[43]D. Gérard, A. Devilez, H. Aouani, B. Stout, N. Bonod, J. Wenger, E. Popov, and H. Rigneault, "Efficient excitation and collection of single-molecule fluorescence close to a dielectric microsphere," J. Opt. Soc. Am. B **26**, 1473–1478 (2009).
[44]H. Aouani, F. Deiss, J. Wenger, P. Ferrand, N. Sojic, and H. Rigneault, "Optical-fiber-microsphere for remote fluorescence correlation spectroscopy," Opt. Express **17**, 19085–19092 (2009).
[45]P. Ghenuche, J. de Torres, P. Ferrand, and J. Wenger, "Multi-focus parallel detection of fluorescent molecules at picomolar concentration with photonic nanojets arrays," Appl. Phys. Lett. **105**, 131102 (2014).
[46]Y. Yan, Y. Zeng, Y. Wu, Y. Zhao, L. Ji, Y. Jiang, and L. Li, "Ten-fold enhancement of ZnO thin film ultraviolet-luminescence by dielectric microsphere arrays," Opt. Express **22**, 23552–23564 (2014).
[47]B. Rolly, B. Stout, S. Bidault, and N. Bonod, "Crucial role of the emitter–particle distance on the directivity of optical antennas," Opt. Lett. **36**, 3368–3370 (2011).
[48]N. Bonod, A. Devilez, B. Rolly, S. Bidault, and B. Stout, "Ultracompact and unidirectional metallic antennas," Phys. Rev. B **82**, 115429 (2010).
[49]J. Li, A. Salandrino, and N. Engheta, "Shaping light beams in the nanometer scale: A Yagi-Uda nanoantenna in the optical domain," Phys. Rev. B **76**, 245403 (2007).
[50]T. H. Taminiau, F. D. Stefani, and N. F. van Hulst, "Enhanced directional excitation and emission of single emitters by a nano-optical Yagi-Uda antenna," Opt. Express **16**, 10858–10866 (2008).
[51]A. G. Curto, G. Volpe, T. H. Taminiau, M. P. Kreuzer, R. Quidant, and N. F. van Hulst, "Unidirectional emission of a quantum dot coupled to a nano-antenna," Science **329**, 930–933 (2010).
[52]M. Ramezani, A. Casadei, G. Grzela, F. Matteini, G. Tutuncuoglu, D. Ruffer, A. Fontcuberta i Morral, and J. Gomez Rivas, "Hybrid semiconductor nanowire–metallic Yagi-Uda antennas," Nano Lett. **15**, 4889–4895 (2015).
[53]A. Krasnok, A. Miroshnichenko, P. Belov, and Y. Kivshar, "Huygens optical elements and Yagi–Uda nanoantennas based on dielectric nanoparticles," JETP Lett. **94**, 593–598 (2011).
[54]A. E. Krasnok, A. E. Miroshnichenko, P. A. Belov, and Y. S. Kivshar, "All-dielectric optical nanoantennas," Opt. Express **20**, 20599–20604 (2012).
[55]B. Rolly, B. Stout, and N. Bonod, "Boosting the directivity of optical antennas with magnetic and electric dipolar resonant particles," Opt. Express **20**, 20376–20386 (2012).
[56]M. Peter, A. Hildebrandt, C. Schlickriede, K. Gharib, T. Zentgraf, J. Forstner, and S. Linden, "Directional emission from dielectric leaky-wave nanoantennas," Nano Lett. **17**, 4178–4183 (2017).
[57]A. F. Cihan, A. G. Curto, S. Raza, P. G. Kik, and M. L. Brongersma, "Silicon Mie resonators for highly directional light emission from monolayer MoS_2," Nat. Photonics **12**, 284 (2018).
[58]J. Ho, Y. H. Fu, Z. Dong, R. Paniagua-Dominguez, E. H. Koay, Y. F. Yu, V. Valuckas, A. I. Kuznetsov, and J. K. Yang, "Highly directive hybrid metal–dielectric Yagi-Uda nanoantennas," ACS Nano **12**, 8616–8624 (2018).
[59]M. Kerker, D.-S. Wang, and C. L. Giles, "Electromagnetic scattering by magnetic spheres," J. Opt. Soc. Am. **73**, 765–767 (1983).
[60]R. Gomez-Medina, B. Garcia-Camara, I. Suarez-Lacalle, F. Gonzalez, F. Moreno, M. Nieto-Vesperinas, and J. J. Saenz, "Electric and magnetic dipolar response of germanium nanospheres: Interference effects, scattering anisotropy, and optical forces," J. Nanophotonics **5**, 053512 (2011).
[61]M. Nieto-Vesperinas, R. Gomez-Medina, and J. J. Saenz, "Angle-suppressed scattering and optical forces on submicrometer dielectric particles," J. Opt. Soc. Am. A **28**, 54–60 (2011).
[62]I. M. Hancu, A. G. Curto, M. Castro-López, M. Kuttge, and N. F. van Hulst, "Multipolar interference for directed light emission," Nano Lett. **14**, 166–171 (2013).
[63]T. Coenen, F. B. Arango, A. F. Koenderink, and A. Polman, "Directional emission from a single plasmonic scatterer," Nat. Commun. **5**, 3250 (2014).
[64]J. Proust, N. Bonod, J. Grand, and B. Gallas, "Optical monitoring of the magnetoelectric coupling in individual plasmonic scatterers," ACS Photonics **3**, 1581–1588 (2016).
[65]M. Dubois, L. Leroi, Z. Raolison, R. Abdeddaim, T. Antonakakis, J. de Rosny, A. Vignaud, P. Sabouroux, E. Georget, and B. Larrat *et al.*, "Kerker effect in ultrahigh-field magnetic resonance imaging," Phys. Rev. X **8**, 031083 (2018).
[66]R. D. Richtmyer, "Dielectric resonators," J. Appl. Phys. **10**, 391–398 (1939).
[67]R. K. Mongia and P. Bhartia, "Dielectric resonator antennas—A review and general design relations for resonant frequency and bandwidth," Int. J. Microwave Millimeter-Wave Comput. Aided Eng. **4**, 230 (1994).
[68]D. S. Filonov, A. E. Krasnok, A. P. Slobozhanyuk, P. V. Kapitanova, E. A. Nenasheva, Y. S. Kivshar, and P. A. Belov, "Experimental verification of the concept of all-dielectric nanoantennas," Appl. Phys. Lett. **100**, 201113 (2012).

[69]B. Rolly, J.-M. Geffrin, R. Abdeddaim, B. Stout, and N. Bonod, "Controllable emission of a dipolar source coupled with a magneto-dielectric resonant subwavelength scatterer," Sci. Rep. **3**, 3063 (2013).
[70]A. E. Krasnok, D. S. Filonov, C. R. Simovski, Y. S. Kivshar, and P. A. Belov, "Experimental demonstration of superdirective dielectric antenna," Appl. Phys. Lett. **104**, 133502 (2014).
[71]A. E. Krasnok, C. R. Simovski, P. A. Belov, and Y. S. Kivshar, "Superdirective dielectric nanoantennas," Nanoscale **6**, 7354–7361 (2014).
[72]A. Krasnok, S. Lepeshov, and A. Alú, "Nanophotonics with 2D transition metal dichalcogenides," Opt. Express **26**, 15972–15994 (2018).
[73]S. Lepeshov, A. Krasnok, and A. Alù, "Enhanced excitation and emission from 2d transition metal dichalcogenides with all-dielectric nanoantennas," Nanotechnology **30**, 254004 (2019).
[74]P. R. Wiecha, A. Cuche, A. Arbouet, C. Girard, G. Colas des Francs, A. Lecestre, G. Larrieu, F. Fournel, V. Larrey, and T. Baron *et al.*, "Strongly directional scattering from dielectric nanowires," ACS Photonics **4**, 2036–2046 (2017).
[75]T. Bucher, A. Vaskin, R. Mupparapu, F. J. Lochner, A. George, K. E. Chong, S. Fasold, C. Neumann, D.-Y. Choi, and F. Eilenberger *et al.*, "Tailoring photoluminescence from MoS_2 monolayers by mie-resonant metasurfaces," ACS Photonics **6**, 1002–1009 (2019).
[76]A. Devilez, B. Stout, and N. Bonod, "Compact metallo-dielectric optical antenna for ultra directional and enhanced radiative emission," ACS Nano **4**, 3390–3396 (2010).
[77]X. Zeng, W. Yu, P. Yao, Z. Xi, Y. Lu, and P. Wang, "Metallo-dielectric hybrid antenna for high purcell factor and radiation efficiency," Opt. Express **22**, 14517–14523 (2014).
[78]M. Decker, T. Pertsch, and I. Staude, "Strong coupling in hybrid metal–dielectric nanoresonators," Philos. Trans. R. Soc. A **375**, 20160312 (2017).
[79]S. Sun, M. Li, Q. Du, C. E. Png, and P. Bai, "Metal–dielectric hybrid dimer nanoantenna: Coupling between surface plasmons and dielectric resonances for fluorescence enhancement," J. Phys. Chem. C **121**, 12871–12884 (2017).
[80]A. Bonakdar and H. Mohseni, "Hybrid optical antenna with high directivity gain," Opt. Lett. **38**, 2726–2728 (2013).
[81]F. Bigourdan, F. Marquier, J.-P. Hugonin, and J.-J. Greffet, "Design of highly efficient metallo-dielectric patch antennas for single-photon emission," Opt. Express **22**, 2337–2347 (2014).
[82]E. Rusak, I. Staude, M. Decker, J. Sautter, A. E. Miroshnichenko, D. A. Powell, D. N. Neshev, and Y. S. Kivshar, "Hybrid nanoantennas for directional emission enhancement," Appl. Phys. Lett. **105**, 221109 (2014).
[83]P. Bharadwaj, B. Deutsch, and L. Novotny, "Optical antennas," Adv. Opt. Photonics **1**, 438–483 (2009).
[84]M. P. Busson, B. Rolly, B. Stout, N. Bonod, and S. Bidault, "Accelerated single photon emission from dye molecule-driven nanoantennas assembled on DNA," Nat. Commun. **3**, 962 (2012).
[85]G. Acuna, F. Möller, P. Holzmeister, S. Beater, B. Lalkens, and P. Tinnefeld, "Fluorescence enhancement at docking sites of DNA-directed self-assembled nanoantennas," Science **338**, 506–510 (2012).
[86]D. Punj, M. Mivelle, S. B. Moparthi, T. S. Van Zanten, H. Rigneault, N. F. Van Hulst, M. F. García-Parajó, and J. Wenger, "A plasmonic antenna-in-box platform for enhanced single-molecule analysis at micromolar concentrations," Nat. Nanotechnol. **8**, 512 (2013).
[87]M. Sigalas, D. Fattal, R. Williams, S. Wang, and R. Beausoleil, "Electric field enhancement between two Si microdisks," Opt. Express **15**, 14711–14716 (2007).
[88]R. M. Bakker, D. Permyakov, Y. F. Yu, D. Markovich, R. Paniagua-Domínguez, L. Gonzaga, A. Samusev, Y. Kivshar, B. Luk'yanchuk, and A. I. Kuznetsov, "Magnetic and electric hotspots with silicon nanodimers," Nano Lett. **15**, 2137–2142 (2015).
[89]R. Regmi, J. Berthelot, P. M. Winkler, M. Mivelle, J. Proust, F. Bedu, I. Ozerov, T. Begou, J. Lumeau, and H. Rigneault *et al.*, "All-dielectric silicon nanogap antennas to enhance the fluorescence of single molecules," Nano Lett. **16**, 5143–5151 (2016).
[90]D. Bouchet, M. Mivelle, J. Proust, B. Gallas, I. Ozerov, M. F. Garcia-Parajo, A. Gulinatti, I. Rech, Y. De Wilde, and N. Bonod *et al.*, "Enhancement and inhibition of spontaneous photon emission by resonant silicon nanoantennas," Phys. Rev. Appl. **6**, 064016 (2016).
[91]J. Bohn, T. Bucher, K. E. Chong, A. Komar, D.-Y. Choi, D. N. Neshev, Y. S. Kivshar, T. Pertsch, and I. Staude, "Active tuning of spontaneous emission by Mie-resonant dielectric metasurfaces," Nano Lett. **18**, 3461–3465 (2018).
[92]V. Rutckaia, F. Heyroth, A. Novikov, M. Shaleev, M. Petrov, and J. Schilling, "Quantum dot emission driven by Mie resonances in silicon nanostructures," Nano Lett. **17**, 6886–6892 (2017).
[93]E. Y. Tiguntseva, G. P. Zograf, F. E. Komissarenko, D. A. Zuev, A. A. Zakhidov, S. V. Makarov, and Y. S. Kivshar, "Light-emitting halide perovskite nanoantennas," Nano Lett. **18**, 1185–1190 (2018).
[94]A. Vaskin, J. Bohn, K. E. Chong, T. Bucher, M. Zilk, D.-Y. Choi, D. N. Neshev, Y. S. Kivshar, T. Pertsch, and I. Staude, "Directional and spectral shaping of light emission with Mie-resonant silicon nanoantenna arrays," ACS Photonics **5**, 1359–1364 (2018).
[95]H. Kallel, A. Arbouet, M. Carrada, G. Ben Assayag, A. Chehaidar, P. Periwal, T. Baron, P. Normand, and V. Paillard, "Photoluminescence enhancement of silicon nanocrystals placed in the near field of a silicon nanowire," Phys. Rev. B **88**, 081302 (2013).
[96]M. Caldarola, P. Albella, E. Cortés, M. Rahmani, T. Roschuk, G. Grinblat, R. F. Oulton, A. V. Bragas, and S. A. Maier, "Non-plasmonic nanoantennas for surface enhanced spectroscopies with ultra-low heat conversion," Nat. Commun. **6**, 7915 (2015).
[97]D. G. Baranov, D. A. Zuev, S. I. Lepeshov, O. V. Kotov, A. E. Krasnok, A. B. Evlyukhin, and B. N. Chichkov, "All-dielectric nanophotonics: The quest for better materials and fabrication techniques," Optica **4**, 814–825 (2017).
[98]J. Cambiasso, G. Grinblat, Y. Li, A. Rakovich, E. Cortés, and S. A. Maier, "Bridging the gap between dielectric nanophotonics and the visible regime with effectively lossless gallium phosphide antennas," Nano Lett. **17**, 1219–1225 (2017).
[99]I. Staude, V. V. Khardikov, N. T. Fofang, S. Liu, M. Decker, D. N. Neshev, T. S. Luk, I. Brener, and Y. S. Kivshar, "Shaping photoluminescence spectra with magnetoelectric resonances in all-dielectric nanoparticles," ACS Photonics **2**, 172–177 (2015).
[100]M. Iwanaga, "Recent progress in emittance-controlled optical metasurfaces," J. Phys. Conf. Ser. **1092**, 012053, (2018).
[101]X. Zambrana-Puyalto and N. Bonod, "Purcell factor of spherical Mie resonators," Phys. Rev. B **91**, 195422 (2015).
[102]A. S. Zalogina, R. S. Savelev, E. V. Ushakova, G. P. Zograf, F. E. Komissarenko, V. A. Milichko, S. V. Makarov, D. A. Zuev, and I. V. Shadrivov, "Purcell effect in active diamond nanoantennas," Nanoscale **10**, 8721–8727 (2018).
[103]S. Liu, A. Vaskin, S. Addamane, B. Leung, M.-C. Tsai, Y. Yang, P. Vabishchevich, G. A. Keeler, G. T. Wang, and X. He *et al.*, "Light emitting metasurfaces: Simultaneous control of spontaneous emission and far-field radiation," Nano Lett. **18**, 6906–6914 (2018).
[104]H. Mertens, A. F. Koenderink, and A. Polman, "Plasmon-enhanced luminescence near noble-metal nanospheres: Comparison of exact theory and an improved Gersten and Nitzan model," Phys. Rev. B **76**, 115123 (2007).
[105]P. Albella, M. A. Poyli, M. K. Schmidt, S. A. Maier, F. Moreno, J. J. Sáenz, and J. Aizpurua, "Low-loss electric and magnetic field-enhanced spectroscopy with subwavelength silicon dimers," J. Phys. Chem. C **117**, 13573–13584 (2013).
[106]R. G. Hulet, E. S. Hilfer, and D. Kleppner, "Inhibited spontaneous emission by a Rydberg atom," Phys. Rev. Lett. **55**, 2137–2140 (1985).
[107]M. Sanz-Paz, C. Ernandes, J. U. Esparza, G. W. Burr, N. F. van Hulst, A. Maitre, L. Aigouy, T. Gacoin, N. Bonod, and M. F. Garcia-Parajo *et al.*, "Enhancing magnetic light emission with all-dielectric optical nanoantennas," Nano Lett. **18**, 3481–3487 (2018).
[108]P. R. Wiecha, C. Majorel, C. Girard, A. Arbouet, B. Masenelli, O. Boisron, A. Lecestre, G. Larrieu, V. Paillard, and A. Cuche, "Enhancement of electric and magnetic dipole transition of rare-earth-doped thin films tailored by high-index dielectric nanostructures," Appl. Opt. **58**, 1682–1690 (2019).
[109]A. Vaskin, S. Mashhadi, M. Steinert, K. E. Chong, D. Keene, S. Nanz, A. Abass, E. Rusak, D.-Y. Choi, I. Fernandez-Corbaton, T. Pertsch, C. Rockstuhl,

M. A. Noginov, Y. S. Kivshar, D. N. Neshev, N. Noginova, and I. Staude, "Manipulation of magnetic dipole emission from Eu^{3+} with Mie-resonant dielectric metasurfaces," Nano Lett. **19**, 1015–1022 (2019).
[110]X. Zambrana-Puyalto and N. Bonod, "Tailoring the chirality of light emission with spherical Si-based antennas," Nanoscale **8**, 10441–10452 (2016).
[111]N. Noginova, G. Zhu, M. Mavy, and M. A. Noginov, "Magnetic dipole based systems for probing optical magnetism," J. Appl. Phys **103**, 07E901 (2008).
[112]N. Noginova, Y. Barnakov, H. Li, and M. A. Noginov, "Effect of metallic surface on electric dipole and magnetic dipole emission transitions in Eu^{3+} doped polymeric film," Opt. Express **17**, 10767–10772 (2009).
[113]X. Ni, G. V. Naik, A. V. Kildishev, Y. Barnakov, A. Boltasseva, and V. M. Shalaev, "Effect of metallic and hyperbolic metamaterial surfaces on electric and magnetic dipole emission transitions," Appl. Phys. B **103**, 553–558 (2011).
[114]S. Karaveli and R. Zia, "Strong enhancement of magnetic dipole emission in a multilevel electronic system," Opt. Lett. **35**, 3318–3320 (2010).
[115]S. Karaveli and R. Zia, "Spectral tuning by selective enhancement of electric and magnetic dipole emission," Phys. Rev. Lett. **106**, 193004 (2011).
[116]K. Drexhage, "Influence of a dielectric interface on fluorescence decay time," J. Lumin. **1**, 693–701 (1970).
[117]R. Kunz and W. Lukosz, "Changes in fluorescence lifetimes induced by variable optical environments," Phys. Rev. B **21**, 4814 (1980).
[118]L. Aigouy, A. Cazé, P. Gredin, M. Mortier, and R. Carminati, "Mapping and quantifying electric and magnetic dipole luminescence at the nanoscale," Phys. Rev. Lett. **113**, 076101 (2014).
[119]R. Hussain, S. S. Kruk, C. E. Bonner, M. A. Noginov, I. Staude, Y. S. Kivshar, N. Noginova, and D. N. Neshev, "Enhancing Eu^{3+} magnetic dipole emission by resonant plasmonic nanostructures," Opt. Lett. **40**, 1659–1662 (2015).
[120]F. T. Rabouw, P. T. Prins, and D. J. Norris, "Europium-doped $NaYf_4$ nanocrystals as probes for the electric and magnetic local density of optical states throughout the visible spectral range," Nano Lett. **16**, 7254–7260 (2016).
[121]D. Li, S. Karaveli, S. Cueff, W. Li, and R. Zia, "Probing the combined electromagnetic local density of optical states with quantum emitters supporting strong electric and magnetic transitions," Phys. Rev. Lett. **121**, 227403 (2018).
[122]M. A. van de Haar, J. van de Groep, B. J. Brenny, and A. Polman, "Controlling magnetic and electric dipole modes in hollow silicon nanocylinders," Opt. Express **24**, 2047–2064 (2016).
[123]T. Feng, Y. Xu, Z. Liang, and W. Zhang, "All-dielectric hollow nanodisk for tailoring magnetic dipole emission," Opt. Lett. **41**, 5011–5014 (2016).
[124]K. V. Baryshnikova, A. Novitsky, A. B. Evlyukhin, and A. S. Shalin, "Magnetic field concentration with coaxial silicon nanocylinders in the optical spectral range," J. Opt. Soc. Am. B **34**, D36–D41 (2017).
[125]J. Li, N. Verellen, and P. Van Dorpe, "Enhancing magnetic dipole emission by a nano-doughnut-shaped silicon disk," ACS Photonics **4**, 1893–1898 (2017).
[126]N. Bonod, S. Bidault, G. W. Burr, and M. Mivelle, "Evolutionary optimization of all-dielectric magnetic nanoantennas," Adv. Opt. Mater. **7**, 1900121 (2019).
[127]S. Cueff, D. F. Li, Y. Zhou, F. J. Wong, J. A. Kurvits, S. Ramanathan, and R. Zia, "Dynamic control of light emission faster than the lifetime limit using vo2 phase-change," Nat. Commun. **6**, 8636 (2015).
[128]R. A. DeCrescent, N. R. Venkatesan, C. J. Dahlman, R. M. Kennard, X. Zhang, W. Li, X. Du, M. L. Chabinyc, R. Zia, and J. A. Schuller, "Bright magnetic dipole radiation from two-dimensional lead-halide perovskites," e-print arXiv:1901.05136 [cond-mat] (2019).
[129]Y. Tang and A. E. Cohen, "Optical chirality and its interaction with matter," Phys. Rev. Lett. **104**, 163901 (2010).
[130]A. García-Etxarri and J. A. Dionne, "Surface-enhanced circular dichroism spectroscopy mediated by nonchiral nanoantennas," Phys. Rev. B **87**, 235409 (2013).
[131]C.-S. Ho, A. Garcia-Etxarri, Y. Zhao, and J. Dionne, "Enhancing enantioselective absorption using dielectric nanospheres," ACS Photonics **4**, 197–203 (2017).
[132]W. Zhang, T. Wu, R. Wang, and X. Zhang, "Amplification of the molecular chiroptical effect by low-loss dielectric nanoantennas," Nanoscale **9**, 5701–5707 (2017).
[133]F. Graf, J. Feis, X. Garcia-Santiago, M. Wegener, C. Rockstuhl, and I. Fernandez-Corbaton, "Achiral, helicity preserving, and resonant structures for enhanced sensing of chiral molecules," ACS Photonics **6**, 482–491 (2019).
[134]M. L. Solomon, J. Hu, M. Lawrence, A. García-Etxarri, and J. A. Dionne, "Enantiospecific optical enhancement of chiral sensing and separation with dielectric metasurfaces," ACS Photonics **6**, 43–49 (2019).
[135]N. Suzuki, Y. Wang, P. Elvati, Z.-B. Qu, K. Kim, S. Jiang, E. Baumeister, J. Lee, B. Yeom, and J. H. Bahng *et al.*, "Chiral graphene quantum dots," ACS Nano **10**, 1744–1755 (2016).
[136]A. I. Shlykov, A. S. Baimuratov, A. V. Baranov, A. V. Fedorov, and I. D. Rukhlenko, "Optically active quantum-dot molecules," Opt. Express **25**, 3811–3825 (2017).
[137]X. Zambrana-Puyalto, I. Fernandez-Corbaton, M. L. Juan, X. Vidal, and G. Molina-Terriza, "Duality symmetry and Kerker conditions," Opt. Lett. **38**, 1857–1859 (2013).
[138]I. Söllner, S. Mahmoodian, S. L. Hansen, L. Midolo, A. Javadi, G. Kiršanskė, T. Pregnolato, H. El-Ella, E. H. Lee, and J. D. Song *et al.*, "Deterministic photon–emitter coupling in chiral photonic circuits," Nat. Nanotechnol. **10**, 775 (2015).
[139]S.-H. Gong, F. Alpeggiani, B. Sciacca, E. C. Garnett, and L. Kuipers, "Nanoscale chiral valley-photon interface through optical spin-orbit coupling," Science **359**, 443–447 (2018).
[140]T. Chervy, S. Azzini, E. Lorchat, S. Wang, Y. Gorodetski, J. A. Hutchison, S. Berciaud, T. W. Ebbesen, and C. Genet, "Room temperature chiral coupling of valley excitons with spin-momentum locked surface plasmons," ACS Photonics **5**, 1281–1287 (2018).
[141]J. Kumar, T. Nakashima, and T. Kawai, "Circularly polarized luminescence in chiral molecules and supramolecular assemblies," J. Phys. Chem. Lett. **6**, 3445–3452 (2015).
[142]G. Longhi, E. Castiglioni, J. Koshoubu, G. Mazzeo, and S. Abbate, "Circularly polarized luminescence: A review of experimental and theoretical aspects," Chirality **28**, 696–707 (2016).
[143]P. R. Wiecha, A. Arbouet, C. Girard, A. Lecestre, G. Larrieu, and V. Paillard, "Evolutionary multi-objective optimization of colour pixels based on dielectric nanoantennas," Nat. Nanotechnol. **12**, 163 (2017).
[144]S. Molesky, Z. Lin, A. Y. Piggott, W. Jin, J. Vucković, and A. W. Rodriguez, "Inverse design in nanophotonics," Nat. Photonics **12**, 659 (2018).
[145]P. R. Wiecha, A. Lecestre, N. Mallet, and G. Larrieu, "Pushing the limits of optical information storage using deep learning," Nat. Nanotechnol. **14**, 237-244 (2019).
[146]R. Verre, D. G. Baranov, B. Munkhbat, J. Cuadra, M. Käll, and T. Shegai, "Transition metal dichalcogenide nanodisks as high-index dielectric Mie nanoresonators," Nat. Nanotechnol. **14**, 679-683 (2019).
[147]M. Noginov, G. Zhu, A. Belgrave, R. Bakker, V. Shalaev, E. Narimanov, S. Stout, E. Herz, T. Suteewong, and U. Wiesner, "Demonstration of a spaser-based nanolaser," Nature **460**, 1110–1112 (2009).
[148]A. K. Yang, T. B. Hoang, M. Dridi, C. Deeb, M. H. Mikkelsen, G. C. Schatz, and T. W. Odom, "Real-time tunable lasing from plasmonic nanocavity arrays," Nat. Commun. **6**, 6939 (2015).
[149]D. Wang, A. Yang, W. Wang, Y. Hua, R. D. Schaller, G. C. Schatz, and T. W. Odom, "Band-edge engineering for controlled multi-modal nanolasing in plasmonic superlattices," Nat. Nanotechnol. **12**, 889 (2017).
[150]T. Hakala, H. Rekola, A. Väkeväinen, J.-P. Martikainen, M. Nečada, A. Moilanen, and P. Törmä, "Lasing in dark and bright modes of a finite-sized plasmonic lattice," Nat. Commun. **8**, 13687 (2017).
[151]A. F. Koenderink, "Plasmon nanocavity array lasers: Cooperating over losses and competing for gain," ACS Nano **13**, 7377-7382 (2019).
[152]E. Y. Tiguntseva, K. L. Koshelev, A. D. Furasova, V. Y. Mikhailovskii, E. V. Ushakova, D. G. Baranov, T. O. Shegai, A. A. Zakhidov, Y. S. Kivshar, and S. V. Makarov, "Single-particle Mie-resonant all-dielectric nanolasers," arXiv:1905.08646 [physics] (2019).
[153]C. W. Hsu, B. Zhen, A. D. Stone, J. D. Joannopoulos, and M. Soljačić, "Bound states in the continuum," Nat. Rev. Mater. **1**, 16048 (2016).

[154]M. V. Rybin, K. L. Koshelev, Z. F. Sadrieva, K. B. Samusev, A. A. Bogdanov, M. F. Limonov, and Y. S. Kivshar, "High-q supercavity modes in subwavelength dielectric resonators," Phys. Rev. Lett. **119**, 243901 (2017).
[155]K. Koshelev, S. Lepeshov, M. Liu, A. Bogdanov, and Y. Kivshar, "Asymmetric metasurfaces with high-q resonances governed by bound states in the continuum," Phys. Rev. Lett. **121**, 193903 (2018).
[156]A. Kodigala, T. Lepetit, Q. Gu, B. Bahari, Y. Fainman, and B. Kanté, "Lasing action from photonic bound states in continuum," Nature **541**, 196–199 (2017).
[157]S. T. Ha, Y. H. Fu, N. K. Emani, Z. Pan, R. M. Bakker, R. Paniagua-Domínguez, and A. I. Kuznetsov, "Directional lasing in resonant semiconductor nanoantenna arrays," Nat. Nanotechnol. **13**, 1042–1048 (2018).